

AD-A236 813



**Technical Report  
909**

# **Passive Equalization of Wideband Communication Systems**

**M.L. Stevens**

**22 March 1991**

---

**Lincoln Laboratory**

**MASSACHUSETTS INSTITUTE OF TECHNOLOGY**

**LEXINGTON, MASSACHUSETTS**

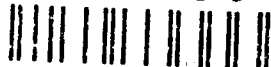


---

**Prepared for the Department of the Air Force  
under Contract F19628-90-C-0002.**

**Approved for public release; distribution is unlimited.**

**91-01770**



This report is based on studies performed at Lincoln Laboratory, a center for research operated by Massachusetts Institute of Technology. The work was sponsored by the Department of the Air Force under Contract F19628-90-C-0002.

This report may be reproduced to satisfy needs of U.S. Government agencies.

The ESD Public Affairs Office has reviewed this report, and it is releasable to the National Technical Information Service, where it will be available to the general public, including foreign nationals.

This technical report has been reviewed and is approved for publication.

FOR THE COMMANDER

*Hugh L. Southall*

Hugh L. Southall, Lt. Col., USAF  
Chief, ESD Lincoln Laboratory Project Office

Non-Lincoln Recipients

PLEASE DO NOT RETURN

Permission is given to destroy this document  
when it is no longer needed.

MASSACHUSETTS INSTITUTE OF TECHNOLOGY  
LINCOLN LABORATORY

PASSIVE EQUALIZATION OF WIDEBAND  
COMMUNICATION SYSTEMS

M.L. STEVENS  
Group 63

TECHNICAL REPORT 909



Accession For	
ALL INFORMATION CONTAINED HEREIN IS UNCLASSIFIED	<input checked="checked" type="checkbox"/>
DATE 10/1/81	<input type="checkbox"/>
BY SP-10	<input type="checkbox"/>
Justification	
By	
Distribution	
Availability Codes	
Avail and/or	
Disc	Special
A-1	

22 MARCH 1991

Approved for public release; distribution is unlimited.

## **ABSTRACT**

This report describes a technique that produces high-performance passive equalization networks for wideband communication systems. The relationship between the time-domain and frequency-domain performance of a simple but important class of networks is derived. The results of this analysis provide an estimate of the precision of equalization required in the frequency domain, given the requirements for waveform quality in the time domain. The effects of equalization magnitude and phase errors on a system transfer function are described, and the optimum weighting function for the least-mean-square-error minimization of magnitude and phase errors is derived. An example is given of the baseband equalization of a 220-Mbit/sec 4-ary FSK optical communication system. High-quality equalization is achieved using this technique over a frequency range of DC to approximately 1 GHz using simple, economical networks. Appendices are provided, describing the APL computer functions that were written to optimize and synthesize the filter hardware.

## **ACKNOWLEDGMENTS**

Steve Alexander blazed the trail of laser equalization, and his work provided the basis for the techniques described here. Steve, Emily Kintzer, and Carl Marangoudakis provided the FM characterization data; David Hodsdon, Doug Marquis, and Charlie Rader provided useful suggestions and/or computer algorithms for the time-domain analysis. Phil Lee built and measured the equalizer hardware.

## TABLE OF CONTENTS

Abstract	iii
Acknowledgments	v
List of Illustrations	ix
List of Tables	xi
 1. INTRODUCTION	 1
 2. A RELATIONSHIP BETWEEN THE TIME-DOMAIN AND FREQUENCY-DOMAIN PERFORMANCE OF A SIMPLE CLASS OF NETWORKS	 3
 3. THE EFFECTS OF MAGNITUDE AND PHASE ERRORS ON A SYSTEM TRANSFER FUNCTION	 9
 4. OPTIMIZATION STRATEGY FOR WIDEBAND EQUALIZERS	 15
 5. PASSIVE EQUALIZER DESIGN FOR A 220-Mbit/sec 4-ary FSK OPTICAL TRANSMITTER	 19
5.1 Design Procedure	21
5.2 System Performance	31
 6. CONCLUSION	 37
 APPENDIX A. LASER EQUALIZATION PROCEDURES	 39
 APPENDIX B. APL COMPUTER FUNCTIONS	 43
 REFERENCES	 47

## LIST OF ILLUSTRATIONS

Figure No.		Page
1	Laser FM transfer characteristic.	1
2	Some simple forms for $e_2(t)$ .	5
3	System passband ripple versus waveform quality.	6
4	High-frequency equalization limits.	7
5	Low-frequency equalization limits.	8
6	A communication system model.	9
7	Magnitude and phase contributions to system error.	11
8	Limits on magnitude and phase errors for equal contribution to system error.	13
9	Laser diode FSK transmitter.	19
10	Laser FM response: (a) laser magnitude and (b) laser phase.	20
11	Modified ideal correction filter response: (a) filter magnitude and (b) filter phase.	21
12	Calculated step response of a laser cascaded with a modified ideal correction filter.	23
13	Optimization using equal weighting of magnitude (decibels) and phase (degrees): (a) magnitude response, (b) phase response, (c) magnitude error, and (d) phase error.	24
14	Optimization using optimum weighting of magnitude (decibels) and phase (degrees): (a) magnitude response, (b) phase response, (c) magnitude error, and (d) phase error.	25
15	Calculated step response using optimized filters: (a) optimization with equal weighting of magnitude and phase ( $F = 0.129$ ) and (b) optimization with optimum weighting of magnitude and phase ( $F = 0.0755$ ).	26
16	Filter topologies: (a) constant resistance and (b) series Z.	26
17	Series Z ladder.	27
18	Equalized laser step response: (a) calculated two-pole equalizer performance, (b) measured two-pole equalizer performance, (c) calculated three-pole equalizer performance, (d) measured three-pole equalizer performance, (e) calculated four-pole equalizer performance, and (f) measured four-pole equalizer performance.	28
19	Element values for a three-pole equalizer: (a) optimized element values and (b) filter design using standard component values.	29

## LIST OF ILLUSTRATIONS (Continued)

Figure No.		Page
20	Physical construction.	30
21	System performance with two-pole equalization: (a) calculated time response, (b) measured 1-MHz square-wave response, (c) measured 10-MHz square-wave response, (d) measured 100-MHz square-wave response, (e) BER at 110 Mbits/sec binary FSK with a $2^{15}-1$ pseudorandom sequence, and (f) BER at 110 Mbits/sec binary FSK with alternating ones and zeros.	32
22	System performance with three-pole equalization: (a) calculated time response, (b) measured 1-MHz square wave, (c) measured 10-MHz square wave, (d) measured 100-MHz square wave, (e) BER at 110 Mbits/sec binary FSK with a $2^{15}-1$ pseudorandom sequence, and (f) BER at 110 Mbits/sec binary FSK with alternating ones and zeros.	33
23	Laser transmitter performance: (a) ASK modulation, (b) FSK laser output (unequalized), and (c) FSK laser output (equalized).	34
24	Laser spectra: (a) unequalized and (b) equalized.	35

## **LIST OF TABLES**

<b>Table No.</b>		<b>Page</b>
1	Magnitude and Phase Errors for Several Values of System Error	12
2	Equalizer Filter Response	30

## 1. INTRODUCTION

High-speed digital communication systems using lasers and fiber optics are now being developed that operate at speeds of hundreds of megabits to gigabits per second. The frequency spectrum of the baseband data in these systems is ultrawideband, covering many decades of frequency. The equalization of such systems to eliminate intersymbol interference (ISI) becomes a challenging problem when the equalizer must operate from DC to several hundred megahertz or several gigahertz. At these speeds, digital filter technology is not yet practical. Predistortion using feedback is possible in theory, but the large loop bandwidths and short loop delays that are required at these speeds make this approach impractical. At the present time, passive equalization is the only approach that appears viable for very wideband systems.

This report describes a design and optimization technique that was developed to create passive networks that perform baseband equalization of a coherent optical communication system utilizing 4-ary FSK modulation at 220 Mbits/sec. The transmitter uses Hitachi channel-substrate-planar (CSP), semiconductor diode lasers that are directly frequency modulated by current injection. The lasers have the typical FM transfer characteristic shown in Figure 1. This equalization problem is particularly difficult because the curve in Figure 1 does not match any simple pole-zero response, and the frequency band of interest stretches from DC to beyond 1 GHz. To achieve the desired system performance goals, this transfer characteristic was equalized to within a few tenths of a decibel in magnitude and a few degrees in phase over many decades of frequency. Keeping the filters simple and rugged in design was desirable, so that the system could be qualified for space applications. The transmitter contains four lasers, each having a unique FM characteristic that requires its own equalizer design. An approach was needed that would result in consistent high-quality equalization for each diode.

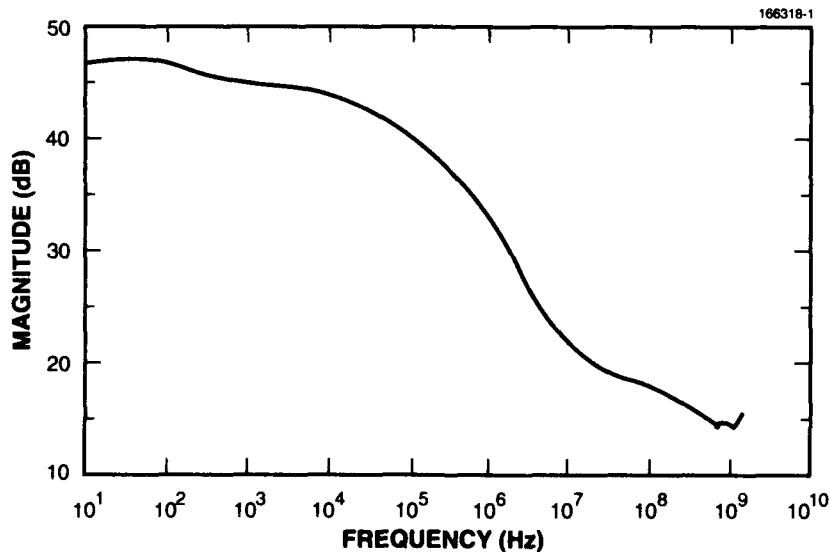


Figure 1. Laser FM transfer characteristic.

The optimization procedure makes use of both the magnitude and phase of a transfer function, where the optimum weighting function for the least-mean-square-error minimization of magnitude and phase has been derived. The optimization procedure operates on the pole and zero values of a transfer function rather than network element values, resulting in a very efficient computer algorithm with wide applications. The optimum weighting function for the minimization of magnitude and phase errors is also applicable to other problems such as image rejection mixer design and adaptive antenna nulling.

A useful relationship is derived between the frequency-domain and time-domain performance of a simple class of networks in Section 2. With the results of this section, the maximum passband ripple requirements and bandwidth of an equalized system can be estimated, given the peak overshoot or undershoot that is acceptable in the time domain. Section 3 derives the optimum weighting function for the minimization of magnitude and phase errors. Section 4 uses the results obtained in Sections 2 and 3 to form a strategy for the optimization of a passive equalizer. Section 5 describes in detail the equalization of a 220-Mbit/sec 4-ary FSK semiconductor diode laser transmitter. Following the summary and conclusions in Section 6, there are two appendices containing the step-by-step optimization procedure and a listing of APL computer functions used in the optimization.

## 2. A RELATIONSHIP BETWEEN THE TIME-DOMAIN AND FREQUENCY-DOMAIN PERFORMANCE OF A SIMPLE CLASS OF NETWORKS

A performance description of a digital system is most easily given in the time domain. It is a fairly simple matter to specify waveform rise time, overshoot, undershoot, and ringing and relate these numbers to system performance. An FSK system, for instance, may switch between several frequencies. The transition time is important because it takes away from the time available to integrate the symbol energy in the presence of noise. The receiver may use a matched filter detection system that does the integration of symbol energy. Any overshoot, undershoot, or ringing may cause the tone to wander out of the matched filter bandwidth. Excessive overshoot or undershoot may even cause the tone to appear in another filter, resulting in intersymbol interference (ISI).

The ability to make precise measurements in the time domain is somewhat limited compared with measurements made in the frequency domain. Time-domain measurements are generally done by oscilloscope. Wideband systems require a very fast oscilloscope that is also susceptible to the noise in the system. In addition, an oscilloscope is a linear device with limited resolution over wide dynamic ranges. It is difficult, for instance, to characterize accurately a fast step that occurs more than 30 dB below the peak of a slowly rising waveform using an oscilloscope. This precise characterization is required to quantify the FM step response of a CSP semiconductor diode laser. In the frequency domain, however, the difference in gain of more than 30 dB between low and high frequencies is easily measurable, the noise bandwidth of the measurement can be narrow, and at the same time measurements over multiple decades of frequencies are easily handled, as shown by the typical measured response in Figure 1.

Unfortunately, the frequency-domain information does not readily reveal what one wants to know, which is how the system will perform in the time domain. A simple way is required to relate the measurements easily made in the frequency domain to the performance that is needed in the time domain. In other words, given the required time-domain performance, the limits of the frequency response of the overall system must be determined.

For the simple case of a system with a single pole and zero, a simple relationship exists between the time-domain and frequency-domain performance.

The time-domain response of a system is given by

$$f_2(t) = f_1(t) * h(t) \quad , \quad (2.1)$$

where  $f_1(t)$  = input waveform,

$f_2(t)$  = output waveform,

$h(t)$  = system impulse response, and

\* = convolution integral.

For a linear system, superposition allows  $h(t)$  to be separated into ideal  $h_I(t)$  and nonideal  $h_E(t)$  parts.

$$f_2(t) = f_1(t) * (h_I(t) + h_E(t)) \quad . \quad (2.2)$$

Let  $f_2(t)$  be composed of the ideal output waveform  $f_1(t)$  (input waveform = output waveform) and an error term  $e_2(t)$ .

$$f_2(t) = f_1(t) + e_2(t) = f_1(t) * (h_I(t) + h_E(t)) \quad (2.3)$$

Equating the ideal and error terms results in

$$f_1(t) = f_1(t) * h_I(t) \quad \text{and} \quad (2.4)$$

$$e_2(t) = f_1(t) * h_E(t) \quad (2.5)$$

The ideal system response  $h_I(t)$  is the unit impulse  $\delta(t)$ . Let  $f_1(t)$  be the unit step  $u(t)$ . Taking the Laplace transform of Equation (2.5),

$$\mathcal{L}e_2(t) = \mathcal{L}u(t) \cdot \mathcal{L}h_E(t) \quad (2.6)$$

$$E_2(s) = \frac{1}{s} \cdot H_E(s) \quad (2.7)$$

$$H_E(s) = sE_2(s) \quad (2.8)$$

Let  $e_2(t)$  take the simple forms shown in Figure 2.

$$e_2(t) = \pm \sigma e^{-\alpha t} \quad \text{or} \quad \pm \sigma (1 - e^{-\alpha t}) \quad (2.9)$$

$$E_2(s) = \pm \sigma \frac{1}{s + \alpha} \quad \text{or} \quad \pm \sigma \left( \frac{1}{s} - \frac{1}{s + \alpha} \right) \quad (2.10)$$

$$H_E(s) = \pm \sigma \frac{s}{s + \alpha} \quad \text{or} \quad \pm \sigma \frac{\alpha}{s + \alpha} \quad (2.11)$$

The overall transfer function  $H_T(s)$  includes the ideal transfer function  $H_I = 1$  and the nonideal  $H_E(s)$ .

$$H_T(s) = 1 \pm \sigma \frac{s}{s + \alpha} \quad \text{or} \quad 1 \pm \sigma \frac{\alpha}{s + \alpha} \quad (2.12)$$

The difference between the overall transfer function and the ideal transfer function in decibels is given by

$$20 \log \left| \frac{H_T(s)}{H_I(s)} \right| = 20 \log \left| \frac{s(1 \pm \sigma) + \alpha}{s + \alpha} \right| \quad (2.13)$$

or

$$20 \log \left| \frac{H_T(s)}{H_I(s)} \right| = 20 \log \left| \frac{s + \alpha(1 \pm \sigma)}{s + \alpha} \right| \quad (2.14)$$

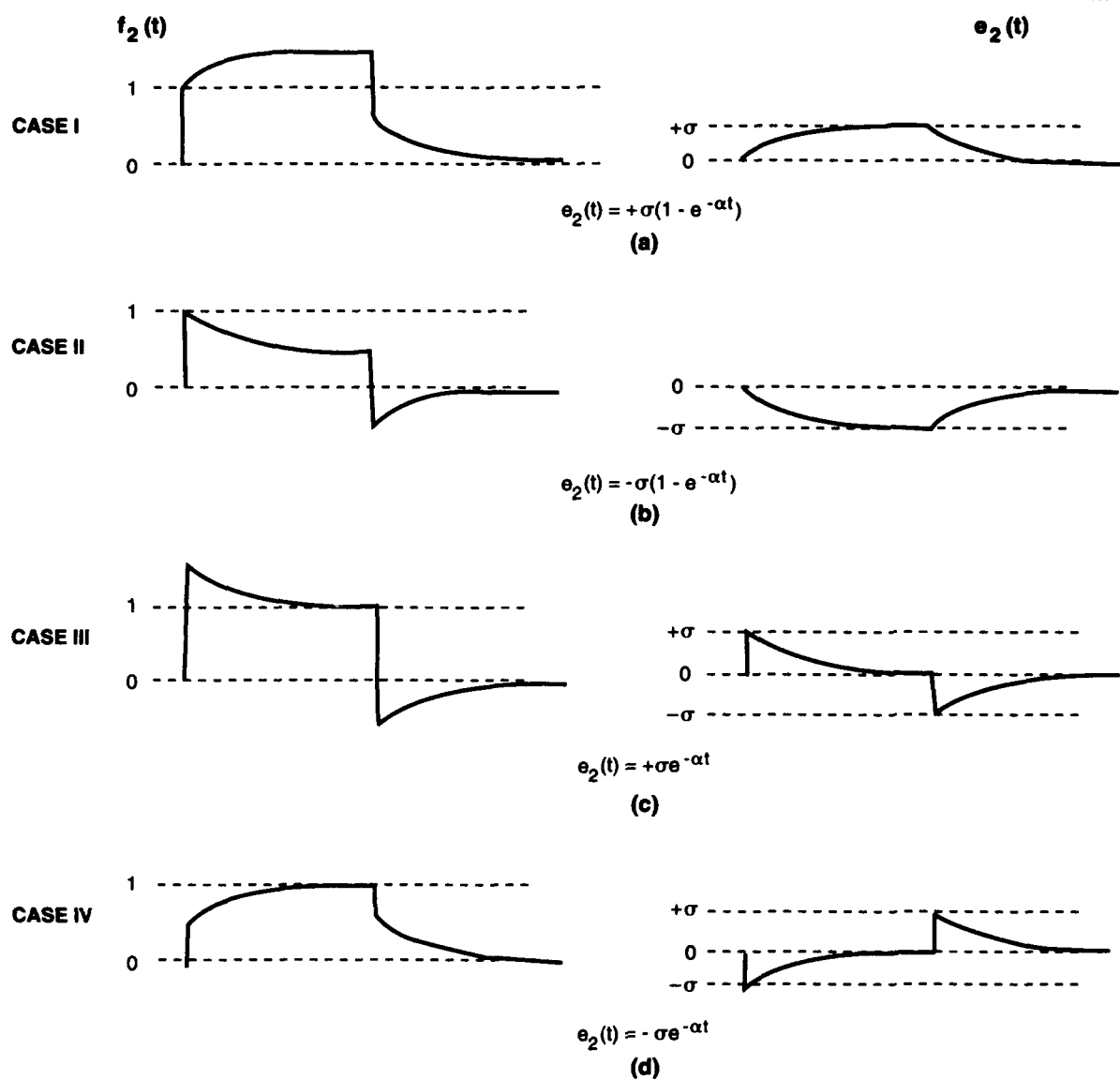


Figure 2. Some simple forms for  $e_2(t)$ .

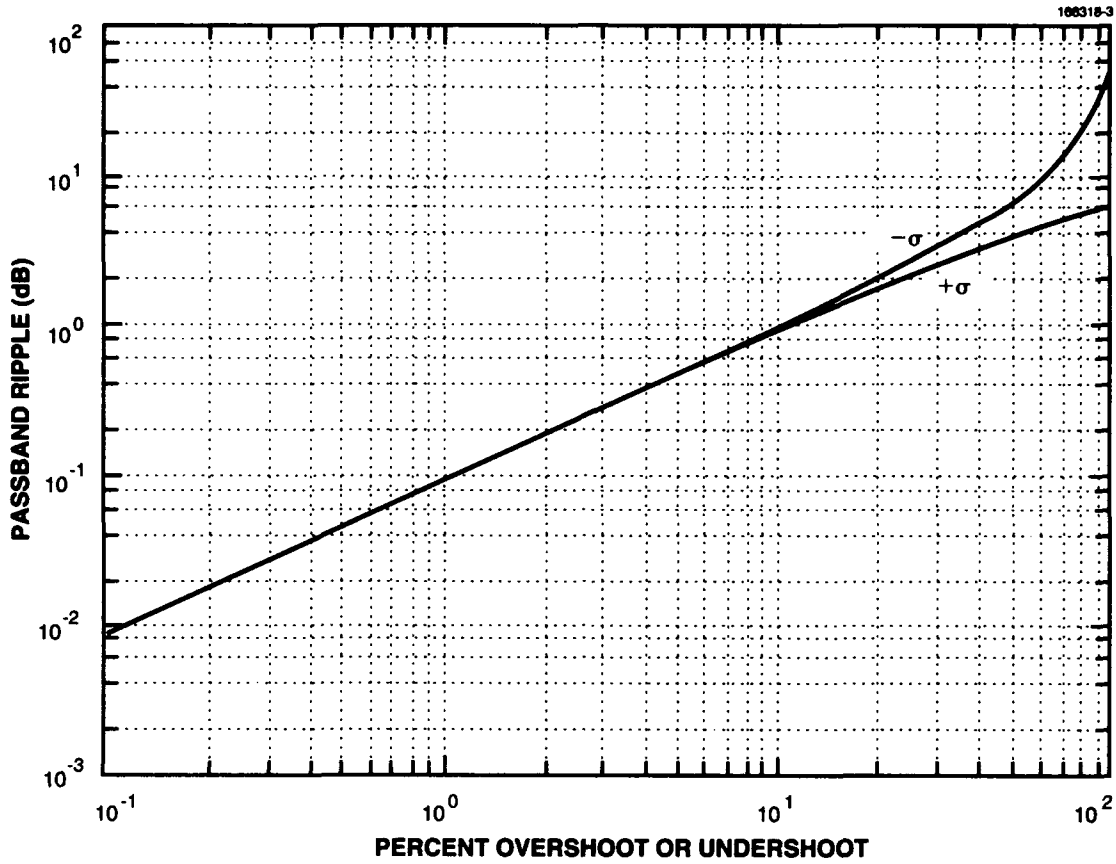


Figure 3. System passband ripple versus waveform quality.

The peak error in the frequency response in either case is

$$\text{ERROR}_{\text{dB}} = 20 \log(1 \pm \sigma) \quad , \quad (2.15)$$

where  $\sigma$  is the fractional error in the time-domain response (i.e., a waveform with 10 percent overshoot has  $\sigma = 0.1$ ).

Figure 3 plots the magnitude of ripple in the frequency response of a system having one of the characteristics shown in Figure 2 as a function of the fractional error in the time domain  $\sigma$ .

The bandwidth requirements in the frequency domain can also be determined from the time-domain specifications. The time-domain specifications of a system will generally have a maximum acceptable rise time. Any overshoot or undershoot that has damped out (to within an acceptable error) during the rise time will not detract from the system performance. In this case the system response  $\sigma$  can deviate from the required passband response,  $\sigma_0$ , according to

$$\pm \sigma = \pm \sigma_0 e^{\alpha T_{\min}} \quad , \quad (2.16)$$

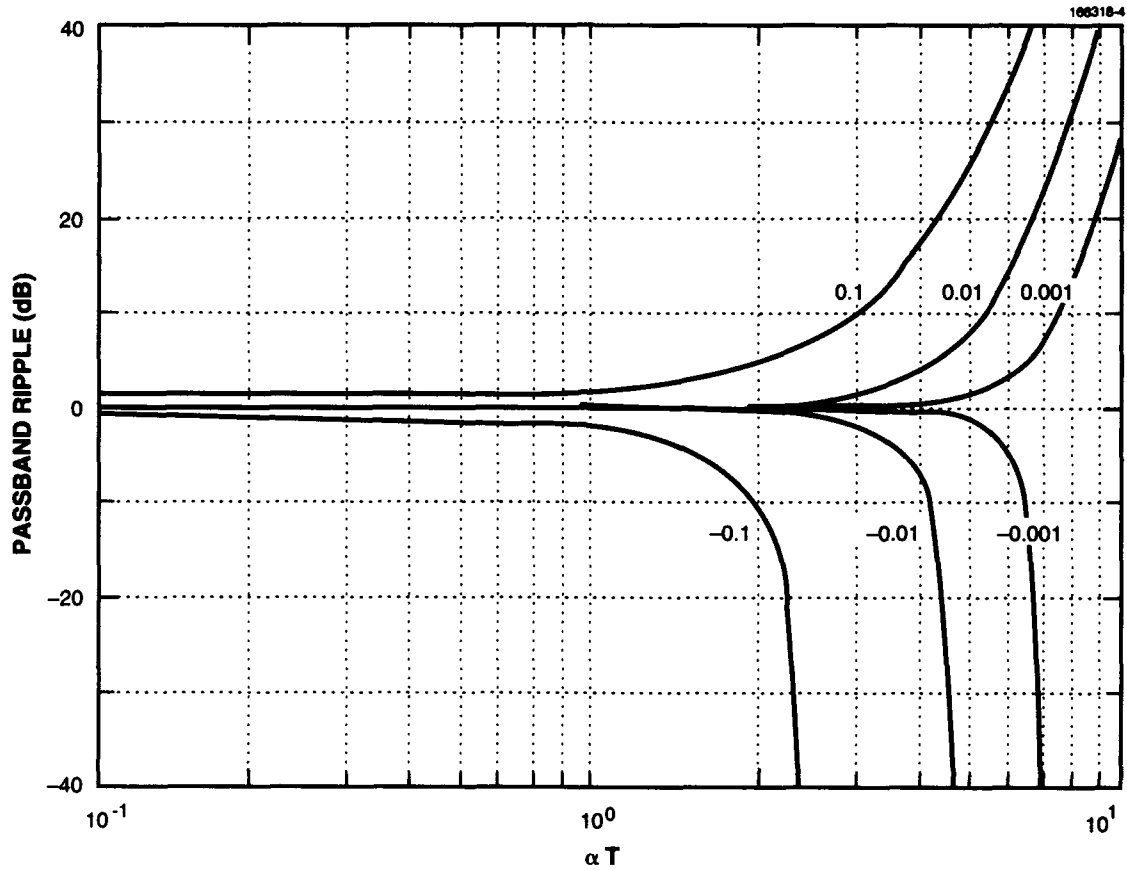


Figure 4. High-frequency equalization limits.

where  $T_{\min}$  is the minimum time of interest in the system. The ripple as a function of  $\alpha T$  is plotted in Figure 4 for several values of  $\sigma_0$ . Figure 4 can be used to determine the minimum upper cutoff frequency of an equalization network. The radian frequency is given by  $\alpha$  where the maximum tolerable error  $\sigma_0$  is given and the minimum time of interest  $T$  is known.

The low-frequency response of an equalization network is determined by

$$\pm\sigma = \pm\sigma_0 \frac{1}{1 - e^{-\alpha T_{\max}}} \quad , \quad (2.17)$$

where  $T_{\max}$  is the maximum time period of interest in the system. The ripple in magnitude response as a function of  $\alpha T$  is plotted in Figure 5 for the low-frequency case.

The preceding discussion provides an important band-limiting of the problem that allows the equalization of a system to be optimized only over the important frequency band. Outside this band, the system may be allowed to deviate from the ideal passband response according to Figure 4 at high frequencies and according to Figure 5 at low frequencies.

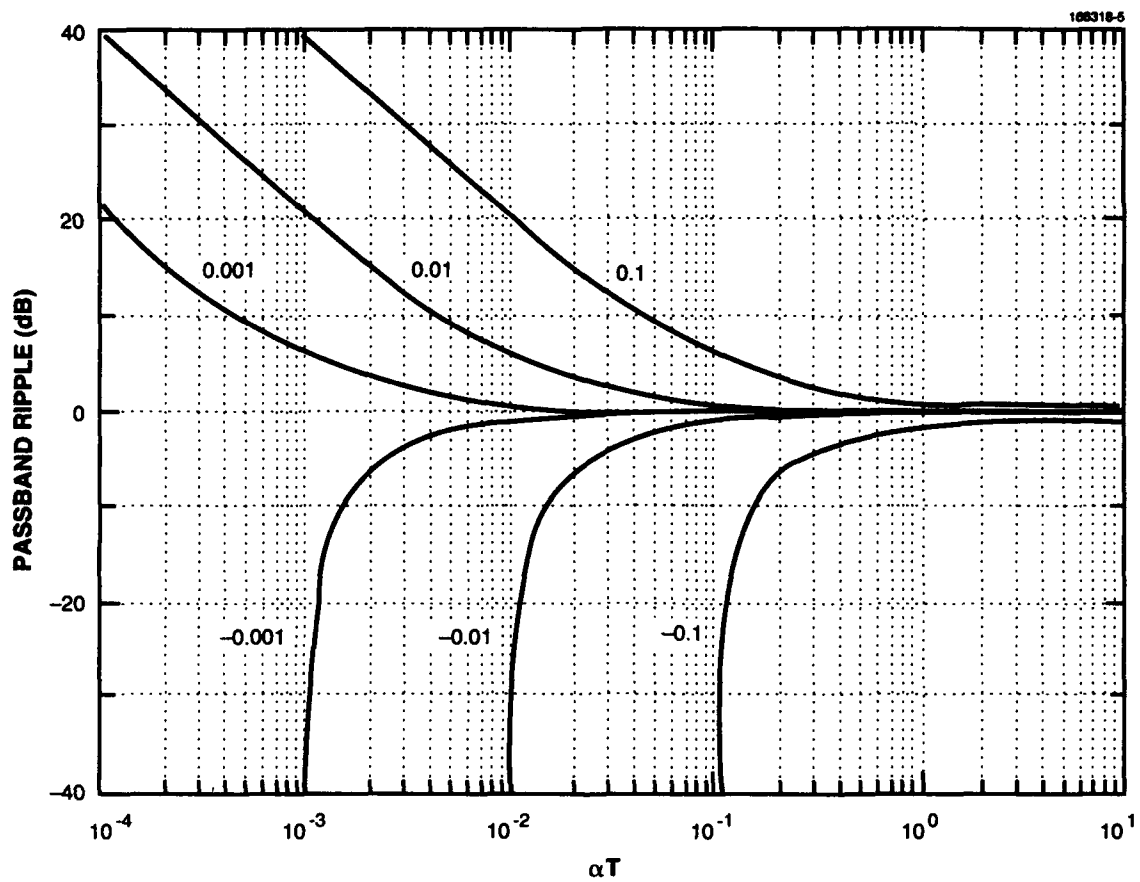


Figure 5. Low-frequency equalization limits.

### 3. THE EFFECTS OF MAGNITUDE AND PHASE ERRORS ON A SYSTEM TRANSFER FUNCTION

A simple model of an equalized communication system is shown in Figure 6.  $S_E$  is the complex transfer function of the equalization filter in the s-plane, and  $S_L$  is the complex transfer function of the communication path in the s-plane, which could represent, for example, the model of a long cable, microwave, or optical link.

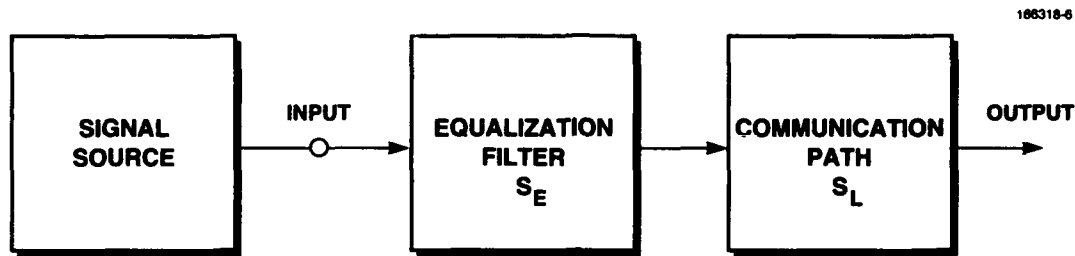


Figure 6. A communication system model.

The overall system transfer function is

$$H_{\text{system}} = S_E \cdot S_L \quad (3.1)$$

The ideal transfer function is

$$H_{\text{system}} = 1 \quad (3.2)$$

in which case, the output will be identical to the input with no waveform distortion.

$$S_L = |S_L| \cdot (\cos \theta + j \sin \theta) \quad \text{and} \quad (3.3)$$

$$S_E = |S_E| \cdot (\cos(-\theta + \varphi) + j \sin(-\theta + \varphi)) \quad (3.4)$$

where  $|S_L|$  is the magnitude of  $S_L$  and  $\theta$  is the phase angle. Likewise,  $|S_E|$  is the magnitude of  $S_E$  and  $(-\theta + \varphi)$  is the phase angle. When  $\varphi = 0$ ,  $S_E$  has the desired ideal phase of  $-\theta$ ;  $\varphi$  therefore represents a phase error term.

The overall transfer function now becomes

$$H_{\text{system}} = S_L \cdot S_E = |S_L| \cdot |S_E| \cdot (\cos \varphi + j \sin \varphi) \quad (3.5)$$

The error in the system transfer function is given by

$$\text{ERROR} = S_L \cdot S_E - 1 \quad (3.6)$$

The magnitude of the squared error is given by

$$|\text{ERROR}|^2 = \left( (S_L \cdot S_E - 1)(S_L \cdot S_E)^* - 1 \right) \quad (3.7)$$

where  $(S_L \cdot S_E)^*$  is a complex conjugate.

$$|\text{ERROR}|^2 = |S_L|^2 \cdot |S_E|^2 - 2|S_L| \cdot |S_E| \cdot \cos \varphi + 1 \quad (3.8)$$

In the ideal case  $|S_E| = 1/|S_L|$  and  $\varphi = 0$ . To study the effects of errors in  $|S_E|$  and  $\varphi$ , let

$$|S_E| = \frac{|1 + \sigma|}{|S_L|} \quad (3.9)$$

where  $-1 \leq \sigma \leq \infty$ , and  $\sigma$  is the fractional error in magnitude.

$$|\text{ERROR}|^2 = \frac{|S_L|^2 \cdot |1 + 2\sigma + \sigma^2|}{|S_L|^2} - \frac{2|S_L| \cdot |1 + \sigma| \cdot \cos \varphi}{|S_L|} + 1 \quad (3.10)$$

$$|\text{ERROR}|^2 = |1 + 2\sigma + \sigma^2| - 2|1 + \sigma| \cdot \cos \varphi + 1 \quad (3.11)$$

Let  $|\text{ERROR}|^2 = \varepsilon$  and solve for  $\sigma$ .

$$\sigma^2 + \sigma(2(1 - \cos \varphi)) + 2(1 - \cos \varphi) - \varepsilon = 0 \quad (3.12)$$

$$\sigma = -(1 - \cos \varphi) \pm \left( (1 - \cos \varphi)^2 - 2(1 - \cos \varphi) + \varepsilon \right)^{\frac{1}{2}} \quad (3.13)$$

If the value of  $\varepsilon$  is known or if  $\varepsilon$  represents a limiting value of system error, then the values of  $\varphi$  and  $\sigma$  that produce the total system error can now be found. Equation (3.13) shows that the possible values of  $\varphi$  are limited to those values that result in real values of  $\sigma$ .

$$(1 - \cos \varphi)^2 - 2(1 - \cos \varphi) + \varepsilon \geq 0 \quad (3.14)$$

or

$$\varepsilon \geq \frac{(1 - \cos 2\varphi)}{2} \quad (3.15)$$

And finally,

$$\cos 2\varphi \geq 1 - 2\varepsilon \quad (3.16)$$

The power series expansion of  $\cos 2\varphi$  is given by

$$\cos 2\varphi = 1 - \frac{4\varphi^2}{2!} + \frac{16\varphi^4}{4!} - \frac{64\varphi^6}{6!} + \dots \quad (3.17)$$

For small values of  $\varphi$  ( $\varphi < 0.5$  rad or  $29^\circ$ ) a good approximation of  $\cos 2\varphi$  is given by the first two terms

$$\cos 2\varphi = 1 - 2\varphi^2 \quad (3.18)$$

Combining Equations (3.16) and (3.18), it is seen that

$$\varphi^2 \leq \epsilon \quad (3.19)$$

or

$$|\varphi_{\text{radians}}| \leq |\text{ERROR}| \quad (3.20)$$

From Equation (3.13), by setting  $\varphi = 0$ , then

$$\sigma = \epsilon^{1/2} \quad (3.21)$$

Letting  $|\varphi|$  take values from 0 to  $|\text{ERROR}|$  it is seen that

$$\sigma \leq |\text{ERROR}| \quad (3.22)$$

Equations (3.20) and (3.22) show that magnitude and phase errors contribute equally to the system error for phase errors less than approximately 0.5 rad. Therefore, system performance should be optimized by minimizing  $\sigma$  and  $\varphi$  using equal weighting (where  $\sigma$  is the dimensionless fractional error in magnitude and  $\varphi$  is the phase error in radians). Equation (3.13) has been plotted in Figure 7 over the allowed range of  $\varphi$  and positive values of  $\sigma$  (negative values greater than or equal to -1 are also of interest) for several values of  $|\text{ERROR}_{\text{dB}}|$ .

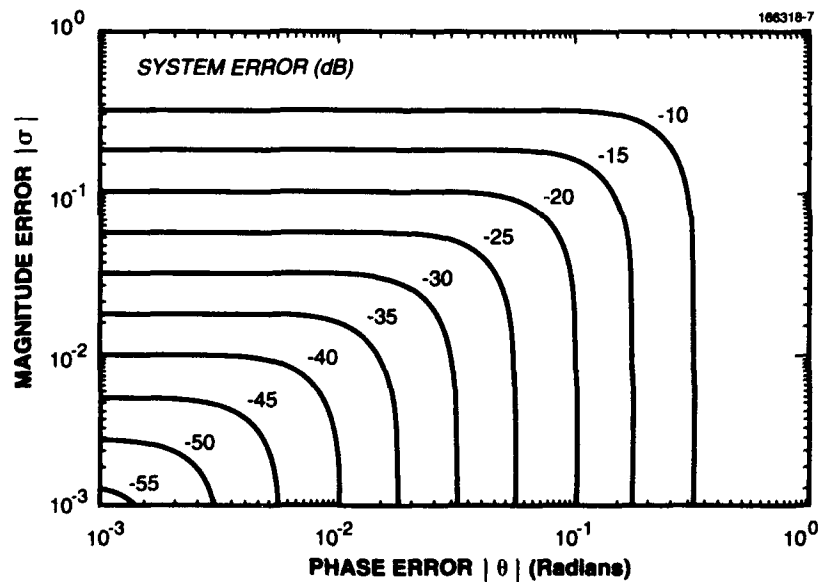


Figure 7. Magnitude and phase contributions to system error.

It is more convenient and generally more effective to optimize the ratio of actual equalization magnitude to ideal equalization magnitude expressed in decibels. This is given by  $20\log_{10}|1 + \sigma|$ , which is the same as the magnitude error given in Equation (2.15), and plotted in Figure 3. Table 1 compares the values of  $|\sigma|$ ,  $|1 + \sigma|$ ,  $20\log_{10}|1 + \sigma|$ , and  $\phi$  in radians and degrees for several values of system error.

**TABLE 1**  
**Magnitude and Phase Errors for Several Values of System Error**

$ \text{ERROR}_{\text{dB}} $	$(\epsilon)^{1/2}$	$\sigma$	$ 1 + \sigma $	$20\log_{10} 1 + \sigma $	$\phi_{\text{rad}}$	$\phi_{\text{deg}}$
-10	0.316	0.316	1.316	2.39	0.316	18.1
-20	0.1	0.1	1.1	0.83	0.1	5.7
-30	0.0316	0.0316	1.0316	0.27	0.0316	1.81
-40	0.01	0.01	1.01	0.086	0.01	0.57
-50	0.00316	0.00316	1.00316	0.027	0.00316	0.18

Table 1 shows that the ratio of magnitude error in decibels and phase error in degrees is approximately 6.7 and is essentially constant for system errors less than -20 dB. This ratio is the appropriate weighting factor for the determination of overall system error that results from both magnitude and phase errors. An appropriate function for the least-mean-square-error minimization of magnitude error in decibels and phase error in degrees is given by

$$E^2 = W_1 \left( M_{\text{dB}} - \underline{M}_{\text{dB}} \right)^2 + W_2 \left( \theta_{\text{deg}} - \underline{\theta}_{\text{deg}} \right)^2 \quad , \quad (3.23)$$

where  $W_1 + W_2 = 1$  and  $W_1/W_2 = 6.7^2$  or

$$W_1 = 0.978,$$

$$W_2 = 0.022,$$

and  $M_{\text{dB}}$  = equalizer magnitude in decibels,  $\underline{M}_{\text{dB}}$  = ideal magnitude in decibels,  $\theta_{\text{deg}}$  = equalizer phase in degrees, and  $\underline{\theta}_{\text{deg}}$  = ideal phase in degrees.

Equation (3.12) can be rewritten in the following form:

$$\sigma^2 + 4\sigma \sin^2 \frac{\phi}{2} + 4 \sin^2 \frac{\phi}{2} = \epsilon \quad . \quad (3.24)$$

As  $\phi/2$  becomes small,  $\sin(\phi/2)$  may be approximated by  $\phi/2$  and Equation (3.24) simplifies to

$$\sigma^2 + \sigma\phi^2 + \phi^2 = \epsilon \quad . \quad (3.25)$$

For  $\sigma$  and  $\varphi \ll 1$ , Equation (3.25) is approximated by

$$\varepsilon = \sigma^2 + \varphi^2 \quad (3.26)$$

When both magnitude error and phase error contribute equally to the system error, the magnitude error  $\sigma$  and phase error in radians  $\varphi$  must be less than or equal to  $(\varepsilon/2)^{1/2}$ . A chart showing the limits on magnitude error in decibels (expressed as  $20\log_{10}|1 + \sigma|$ ) and phase error in degrees as a function of system error in decibels is plotted in Figure 8.

Figures 3, 4, 5, and 8 can be used to estimate the precision necessary to equalize a system transfer function and achieve a required performance in the time domain. Magnitude and phase have been shown to be equally important in contributing to system error. The appropriate weighting factors for minimizing magnitude and phase errors in a system have been derived and can now be used to optimize the design of equalization networks.

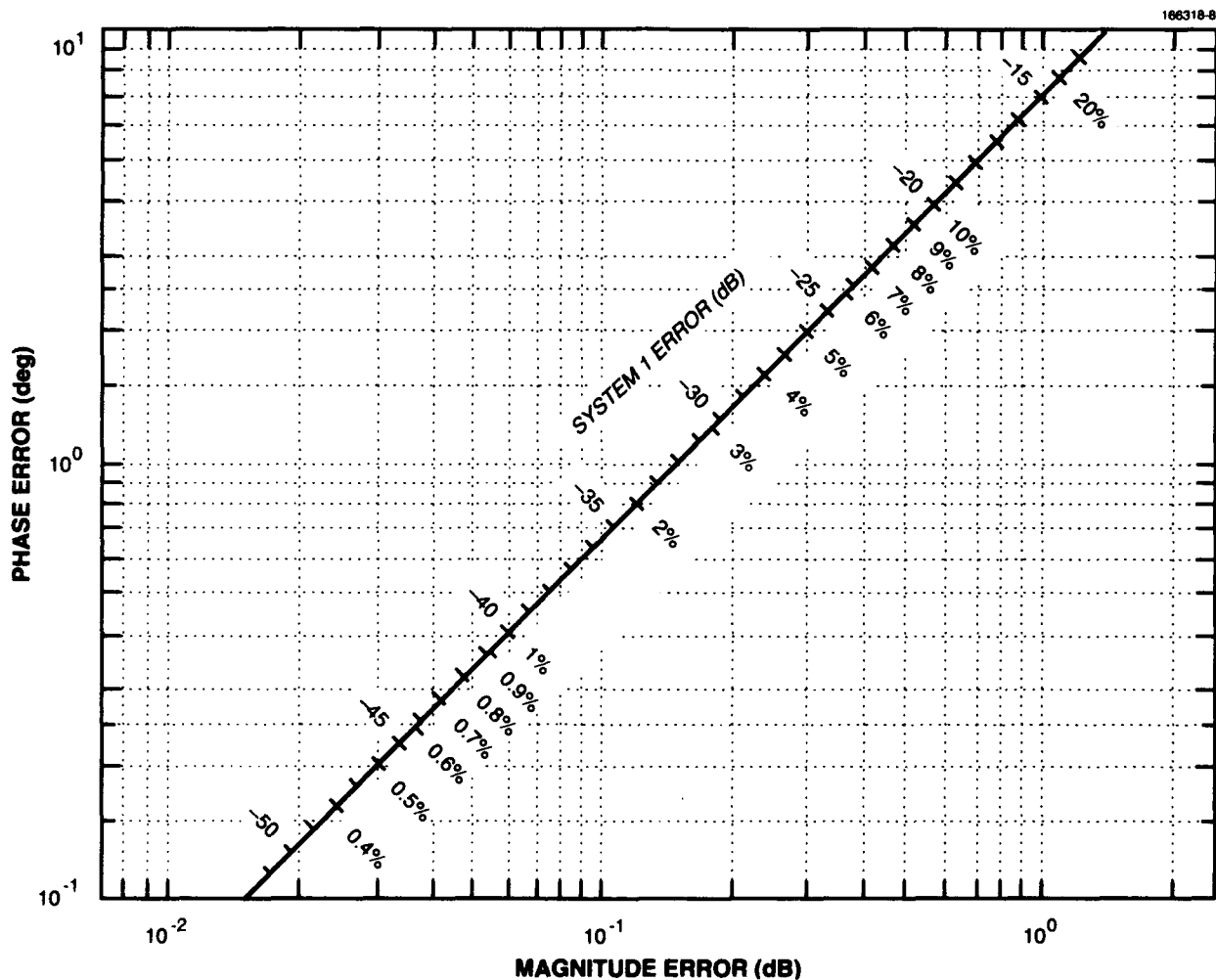


Figure 8. Limits on magnitude and phase errors for equal contribution to system error.

#### 4. OPTIMIZATION STRATEGY FOR WIDEBAND EQUALIZERS

The results in Sections 2 and 3 may now be used to estimate the precision necessary to equalize a system where the time-domain requirements are known. Alternatively, knowing the measured amplitude and phase response of a system versus frequency, we can place limits on the expected performance in the time domain.

The first steps in an optimization strategy are to determine the initial performance of a system and the corrections necessary to achieve the desired performance. For most systems this would involve measuring or calculating the signal spectrum and determining the frequency band of interest, taking into account both the signal spectrum and the rise and fall time requirements. The initial system performance is then determined by measuring the magnitude and phase response versus frequency over the band of interest. Additional measurements, if possible, up to a decade above and below the band of interest will also prove helpful in determining the appropriate out-of-band filter characteristics.

The initial performance could also be measured in the time domain, and this data could then be transformed to the frequency domain by Fourier transform. Because the desired end result is a quality waveform in the time domain, this approach seems more direct than using frequency-domain data. Several problems with this approach exist. First, an equalizer filter will be synthesized in the frequency domain using standard filter synthesis techniques, which forces the problem into the frequency domain whether we start there or not. More importantly, the time domain is a linear domain both in terms of amplitude and time. To characterize a very wideband system adequately requires hundreds or thousands of times as many data points in the time domain using linear sampling than in the frequency domain using logarithmic sampling. As an example, the FM transfer characteristic of a laser was well characterized with 99 logarithmically spaced measurements of magnitude and phase over a frequency band of 10 Hz to 1300 MHz. The same characterization in the time domain would require 130 million data points linearly spaced in the time domain.

From a practical point of view, computer time becomes expensive, and the measured data is generally more noisy and less accurate in the time domain, because of the measurement bandwidths required, than data taken in the frequency domain.

After determining the initial system response, the ideal correction may be calculated that is the inverse of the system response. A system that has a low-pass characteristic will have an ideal correction that is a high-pass characteristic. The ideal correction multiplied by the system response should yield an overall response that is flat in magnitude and zero phase for all frequencies. Unfortunately, the ideal correction will probably violate natural laws, as far as being realizable. The ideal correction for a system with a low-pass characteristic requires a filter that has increasing response with increasing frequency. A realizable filter must approach a transfer function of 1 at high frequencies and have a decreasing response with decreasing frequency below some cutoff frequency. The ideal correction must therefore be modified to a response that is physically realizable. Figures 4 and 5 can be used to determine the appropriate high and low cutoff frequencies for the design.

Before the ideal correction is modified, consider some possible network topologies that could be built to provide the necessary correction over the frequency band of interest. Knowing beforehand the characteristics that the final transfer function must take, the ideal correction can be modified to take on these characteristics at frequencies outside the band of interest. For example, the high-frequency response of a high-pass, minimum-phase filter should approach 0 dB and 0° at high frequencies.

The modified correction now becomes the prototype equalizer characteristic. Modern computer technology, using inverse fast Fourier transform (IFFT) algorithms, can be used to calculate the overall time-domain response of the hypothetical equalizer cascaded with the system to determine whether one is on the right track. The time-domain description of a signal waveform can be transformed using fast Fourier transform (FFT) to the frequency domain, where it is multiplied by the calculated overall system response. The result is then transformed back into the time domain using IFFT. The calculated response of the system in the time domain should compare closely with the signal waveform unless something important was lost in the process of modifying the ideal correction. The modification of the ideal correction can be revised if the calculated time-domain response is unacceptable. The sizes of the FFT and IFFT are determined by the characteristics of the excitation waveform, which can be restricted to provide adequate resolution while maintaining a reasonably sized array of data to transform. Although the system was not measured at the few thousand frequency points that might be required for the IFFT, these points can be accurately interpolated from the logarithmically spaced data points by most modern network analysis programs.

Once the prototype equalizer response has been determined, a first guess of the pole and zero locations of the transfer function can be made. This estimate can be accomplished by plotting the prototype response in Bode plot form and then drawing an asymptotic approximation using the standard rules for drawing Bode plots. A good estimate of the number of poles and zeros that will be required may be obtained at this point by qualitatively comparing the prototype response with the various asymptotic approximations of different order. Most systems will have a response that is exactly modeled by a particular number of poles and zeros. Fewer or more poles or zeros will not work as well and may even cause an optimization routine to diverge. Other systems cannot be exactly modeled by a finite number of poles and zeros. The optimum number in this case is determined experimentally from the characteristics of the data itself and the amount of noise in the measurement. A system with this characteristic is described in the following section.

If accuracies of a few decibels and tens of degrees are adequate, then the Bode approximation may be sufficient, and the filter may be synthesized from the resulting transfer function using standard synthesis techniques. Most systems will require far better accuracies measured in tenths of decibels and a few degrees. The majority of problems will then require an optimization of the equalizer transfer function to minimize the mean-square-error over the band of interest.

An effective optimization algorithm is the Newton-Raphson algorithm for solving systems of  $n$  equations [1].

$$x(j+1) = x(j) - [J(x(j))]^{-1} \times f(x(j)) \quad , \quad (4.1)$$

where  $x(i)$  is the  $i^{\text{th}}$  iteration of  $x$ ,  $J(x(j))$  is the Jacobian matrix of  $f(x)$  evaluated at  $x = x(j)$ , and  $f$  is the function to be minimized. The appropriate function for the least-mean-square minimization of magnitude and phase errors is given by Equation (3.23).

$$E^2 = W_1(M_{\text{dB}} - \underline{M}_{\text{dB}})^2 + W_2(\theta_{\text{deg}} - \underline{\theta}_{\text{deg}})^2$$

In general, Equation (4.1) may be difficult to evaluate directly because of the need to calculate all of the partial derivatives in  $J$  and then form the matrix inverse. If  $f$  has simple derivatives, however, this operation can easily be performed. This is indeed the case if the problem can be limited to transfer functions containing simple real axis poles and zeros. Reducing many complex equalization problems to this form may be possible by adding a filter to the unequalized system that reduces the overall transfer function to a slope of less than 6 dB per octave. Then a final filter can be optimized with alternating poles and zeros that will compensate for the remaining error in the transfer function.

$M_{\text{dB}}$  in Equation (3.23) will then take the form

$$M_{\text{dB}} = 10 \log_{10} \prod_{n=1}^N \frac{\omega^2 + z_n^2}{\omega^2 + p_n^2}, \quad (4.2)$$

where  $z_1, z_2, z_3, \dots$  and  $p_1, p_2, p_3, \dots$  are simple real axis zeros and poles.

$\theta_{\text{deg}}$  in Equation (3.23) will take the form

$$\theta_{\text{deg}} = \frac{180}{\pi} \left[ \sum_{n=1}^N \tan^{-1} \frac{\omega}{z_n} - \sum_{n=1}^N \tan^{-1} \frac{\omega}{p_n} \right] \quad (4.3)$$

The partial derivatives of Equation (3.23) are given by

$$\frac{\partial E^2}{\partial x_n} = 2W_1(M_{\text{dB}} - \underline{M}_{\text{dB}}) \frac{\partial M_{\text{dB}}}{\partial x_n} + 2W_2(\theta_{\text{deg}} - \underline{\theta}_{\text{deg}}) \frac{\partial \theta_{\text{deg}}}{\partial x_n}, \quad (4.4)$$

where  $x_n$  is a pole or zero in the transfer function. The derivatives of  $M_{\text{dB}}$  and  $\theta_{\text{deg}}$  for poles and zeros are

$$\frac{\partial M_{\text{dB}}}{\partial z_n} = \frac{10}{\ln 10} \frac{2z_n}{\omega^2 + z_n^2} \quad (4.5)$$

$$\frac{\partial M_{\text{dB}}}{\partial p_n} = -\frac{10}{\ln 10} \frac{2p_n}{\omega^2 + p_n^2} \quad (4.6)$$

$$\frac{\partial \theta_{\text{deg}}}{\partial z_n} = -\frac{180}{\pi} \frac{\omega}{\omega^2 + z_n^2} \quad (4.7)$$

$$\frac{\partial \theta_{\text{deg}}}{\partial p_n} = \frac{180}{\pi} \frac{\omega}{\omega^2 + p_n^2} \quad (4.8)$$

Equation (4.4) must be solved for each pole and each zero at every frequency point of interest. A solution is possible if the number of frequency points equals the sum of the poles and zeros in the transfer function. This problem would lead to an exact solution at just those frequencies, whereas the transfer function may deviate markedly from the ideal correction at frequencies between these points. For this reason, the optimization will be more accurate if the problem is overspecified, with more equations than there are unknowns, and a best-fit compromise is found for all the solutions. The APL computer language is ideally suited to solve problems of this type with primitive functions that operate on  $n$ -dimensional arrays of data. Appendix B contains a listing of APL functions that were written to solve this problem.

If the problem is overspecified, there is a high probability that local minima may exist and that the global minimum may not be zero. In this situation, the Newton-Raphson algorithm will not converge. As the solution approaches a local or global minimum (which is nonzero), the derivatives will all approach zero, but the step computed for each unknown will become very large. To prevent the optimization from diverging, a scalar multiplier may be included in Equation (4.1) that has a value less than or equal to 1.

$$x(j+1) = x(j) - k[J(x(j))]^{-1} \times f(x(j)) \quad (4.9)$$

At the start of a minimization,  $k$  is set to 1, allowing the algorithm to approach a minimum with maximum speed. As soon as the solution begins to diverge,  $k$  is successively reduced in value to 1/2, 1/4, 1/8, ... until convergence is again established. The optimization quits when either the error becomes zero (very unlikely) or the change in every pole and zero is less than 0.01 percent (or some other arbitrary limit).

Once the optimization has been completed, a filter can be synthesized from the resulting transfer function. FFT and IFFT can be used to calculate the time-domain performance of the equalized system.

An optimization strategy has been described that will be used in the following section to design equalizers for a 220-Mbit/sec FSK coherent optical communication system.

## 5. PASSIVE EQUALIZER DESIGN FOR A 220-MBIT/SEC 4-ARY FSK OPTICAL TRANSMITTER

A simplified block diagram of an FSK optical transmitter is shown in Figure 9. The modulator produces an m-ary amplitude-shift-keyed (ASK) current waveform that is superimposed on the DC bias current of the laser. The laser behaves as a voltage-controlled oscillator (VCO) (actually current-controlled) and converts the ASK input to frequency-shift-keyed (FSK) modulation on the laser carrier.

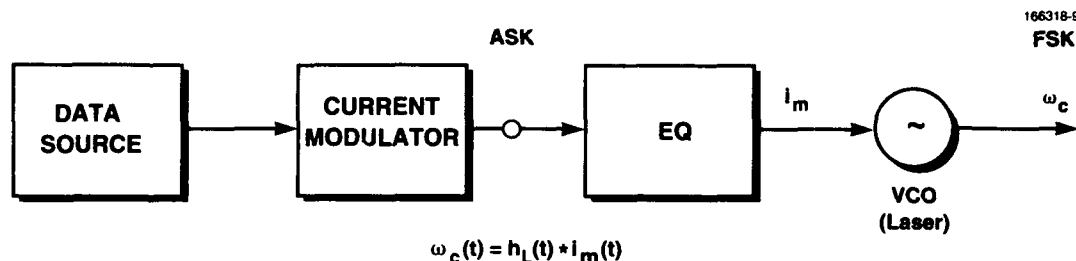


Figure 9. Laser diode FSK transmitter.

The unequalized FM transfer characteristic of a typical Hitachi CSP semiconductor diode laser is shown in Figure 10. The transfer function has been shown to follow a  $1/(s)^{1/2}$  dependence [2] that cannot be exactly modeled by a finite number of poles and zeros. The equalizer design task is therefore to find the minimum number of poles and zeros and their values, which will approximate the inverse of the laser transfer function to the desired accuracy. The desired accuracy is specified only in the time domain and consists of the goal to maintain the FSK output of the laser to within 5 MHz over the duration of a long string of identical symbols. The step size between nonidentical symbols is  $n \times 220$  MHz, where  $n = 1, 2$ , or 3, depending on the actual data sequence.

The allowed variation in frequency represents a  $\sigma$  value of 0.023. Figure 3 gives a corresponding passband ripple value of 0.195 dB. Because phase and magnitude errors both contribute to system error, the equalization precision required to meet the stated goal, from Figure 7, is less than 0.15 dB peak ripple in the magnitude response and  $1^\circ$  deviation from linear phase.

The system passband is determined from the rise-time specification of a 0.5-nsec maximum. The magnitude response of the equalized system can be allowed to increase by 3 dB at an upper cutoff frequency above  $\alpha T = 3$  for a  $\sigma_0$  value of 0.023, resulting in an upper cutoff frequency of  $6 \times 10^9$  rad/sec or 955 MHz. In this particular case, the upper cutoff frequency can be lowered considerably because of the natural compatibility of the high-frequency response characteristics of the laser and the equalizer filter, which both approach a flat response above 100 to 300 MHz. For this reason, no benefit was gained by optimizing the equalization at frequencies above this point.

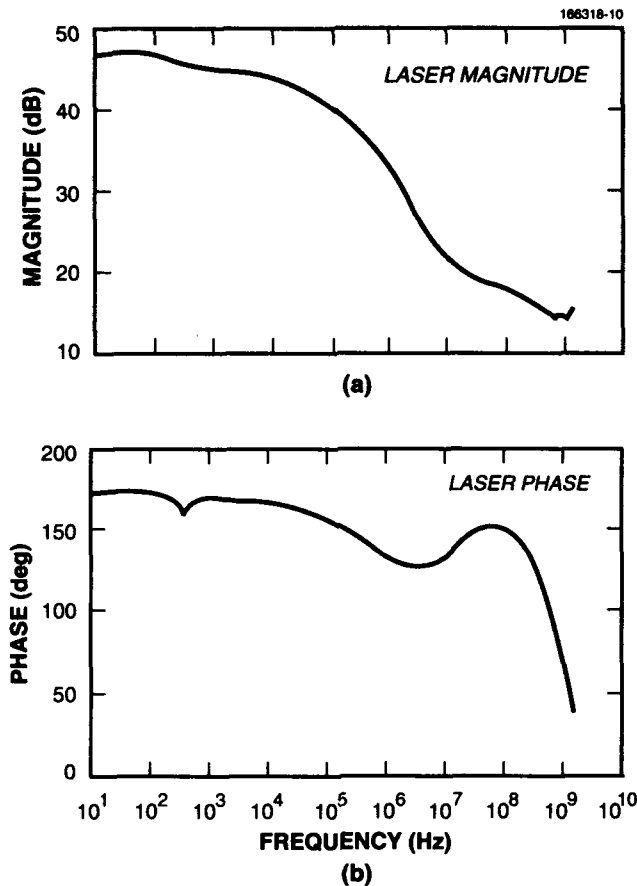


Figure 10. Laser FM response: (a) laser magnitude and (b) laser phase.

The lower cutoff must accommodate the longest string of identical symbols. The system will be tested with a  $2^{15}-1$  pseudorandom sequence containing a maximum of 16 identical symbols. The lowest symbol rate is 13.75 Msymbols/sec, resulting in a  $T_{\min}$  of 1.16  $\mu$ s. A 3-dB variation in magnitude response is allowed at frequencies below  $\alpha T = 0.06$  for a  $\sigma_0$  value of 0.023. This value of  $\alpha T$  results in a lower cutoff below 51.5 krad/sec or 8.2 kHz. The receiver has a frequency tracking loop that tracks out frequency modulation components below 10 kHz, and for this reason, the transmitter equalization was extended only to 10 kHz so that both the transmitter and receiver would have compatible lower limits.

At the outset it was apparent that equalizing the system to within 0.15 dB and  $1^\circ$  from 10 kHz to 300 MHz was probably beyond the current state of the art in laser FM response measurements, primarily because of phase and intensity noise on the laser output. The goal was then to make a "best effort" based on the limited accuracy of the system characterization. At the present time, the accuracy of equalization appears to be limited by noise in the measurement of the FM characteristic of the lasers to approximately  $\pm 1$  dB, which could result in as much as a 25-MHz deviation in the laser output frequency. In practice, however, equalization to better than one-half of this value has been achieved in some cases.

## 5.1 DESIGN PROCEDURE

A filter prototype is created from the measured magnitude and phase of the laser FM transfer characteristic shown in Figure 10. The magnitude response of the filter prototype is created from the magnitude of the measured FM characteristic in decibels by multiplying by -1 and normalizing to 0 dB at the peak of the inverted response. If the laser shows a rise in the response at very high frequencies, the prototype response is forced to 0 dB at frequencies above the peak, as shown in Figure 11(a). Also, if the laser shows a sloping response above 100 to 300 MHz, the data is altered to a flat 0-dB response at these frequencies.

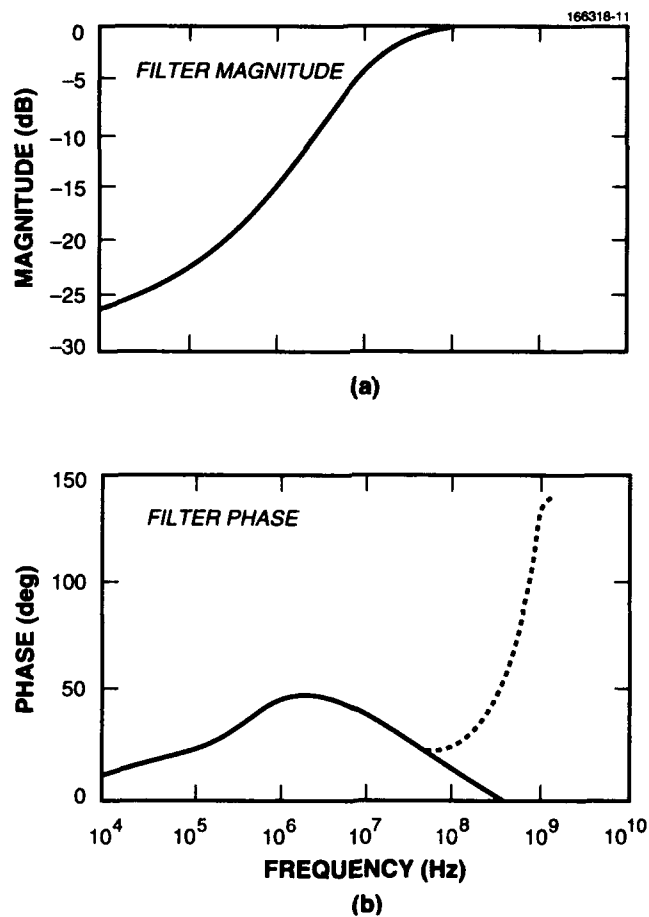


Figure 11. Modified ideal correction filter response: (a) filter magnitude and (b) filter phase.

The lasers have a low-frequency FM response that is 180° out-of-phase with the driving waveform, which means that the frequency of the laser goes down as the current through the junction goes up. Therefore, the phase response of the prototype is subtracted from 180° to produce a minimum-phase-type response for the equalizer that tends to 0° at DC and high frequencies, as shown in Figure 11(b). The relaxation oscillation frequency of the laser, which occurs at approximately 8 GHz, begins to affect the phase response above 100 MHz. This part of the response was found to have little effect on the computed time response and therefore was not included in the filter prototype. This response would have an important effect on higher data-rate systems. The phase response of the prototype is forced to zero at frequencies above approximately 200 MHz by extending the slope of the phase curve from the value at approximately 30 MHz until it reaches 0° at approximately 200 MHz, as shown in Figure 11(b).

A further improvement was made by substituting into the prototype high-frequency phase response the values calculated from

$$\theta_{\text{deg}} = 45 - \frac{180}{2\pi} \tan^{-1} \frac{f}{f_0} \quad , \quad (5.1)$$

where  $f_0$  was chosen to produce the best match to the original prototype phase response. Equation (5.1) approximates the phase response of a network with a  $(s)^{0.5}$  response having an overall phase shift of 45°, rather than the usual 90° and a slope one-half of the usual value. The calculated high-frequency tail was substituted into the prototype response, resulting in a more natural phase characteristic at high frequencies.

At this point, the response of the prototype filter, cascaded with the laser, excited by a 1-MHz square wave, was computed using a 2048-point IFFT. The result should be a high-quality 1-MHz square wave with very minimal distortion; this was verified, as shown in Figure 12. If this is not the case, then either too much of the high-frequency response of the laser was discarded when the prototype filter was created or the laser may have a peculiar response that cannot be well equalized with simple minimum-phase networks. The IFFT becomes a powerful tool to determine what parts of the frequency spectrum are critical to the time-domain performance.

Once the prototype filter has been created, the remaining design problem is to approximate as closely as practical the magnitude and phase response of the prototype filter by determining the pole and zero locations of the transfer function. Initial guesses of the pole-zero locations are determined graphically using a Bode plot. Initial guesses for two-, three-, and four-pole filters were made considering only the prototype response between frequencies of 10 kHz and 1 GHz. Flattening the frequency response above 100 to 300 MHz in the prototype filter and excluding the response below 10 kHz in the optimization forced the poles and zeros into the four most important decades of frequency. This effect reduced the number of poles and zeros required for a given accuracy of performance and therefore reduced the complexity of the equalizer. The initial pole-zero guesses were chosen to yield pole and zero locations that are all real and alternating with a zero located closest to zero frequency. The resulting transfer function is then realized by a simple RC high-pass filter structure.

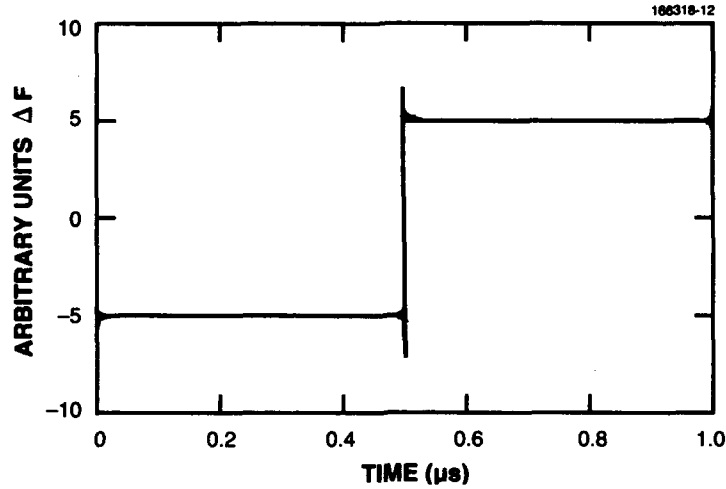


Figure 12. Calculated step response of a laser cascaded with a modified ideal correction filter.

The pole-zero values were computer-optimized by the modified Newton-Raphson algorithm, described in the previous section, which minimizes the sum of the squared errors of magnitude in decibels and phase in degrees summed over the frequencies of interest. In early optimization runs, a comparison was made between optimum weighting of magnitude and phase as defined by Equation (3.23) and equal weighting of magnitude and phase. The optimization using equal weighting is shown in Figure 13, and the optimization using optimum weighting is shown in Figure 14 for the same laser. As expected, optimum weighting results in less error in the magnitude response and greater error in the phase response. According to Figure 8, this is exactly the desired result to minimize the overall system error. Figure 15(a) shows the calculated time-domain performance for the system equalized with equal weighting of magnitude and phase, and Figure 15(b) shows the same system equalized with optimum weighting. A useful figure of merit for the time-domain response is derived by the following:

$$F = \frac{V_{\max} - V_{\min}}{V_{\max} + V_{\min}}, \quad (5.2)$$

where  $V_{\max} - V_{\min}$  is the peak-to-peak value of overshoot minus undershoot in a half-cycle, and  $V_{\max} + V_{\min}$  is a measure of the square-wave amplitude. The figure of merit for equal weighting of magnitude and phase shown in Figure 15(a) is 0.129; optimum weighting, shown in Figure 15(b), results in a much better value of 0.0755.

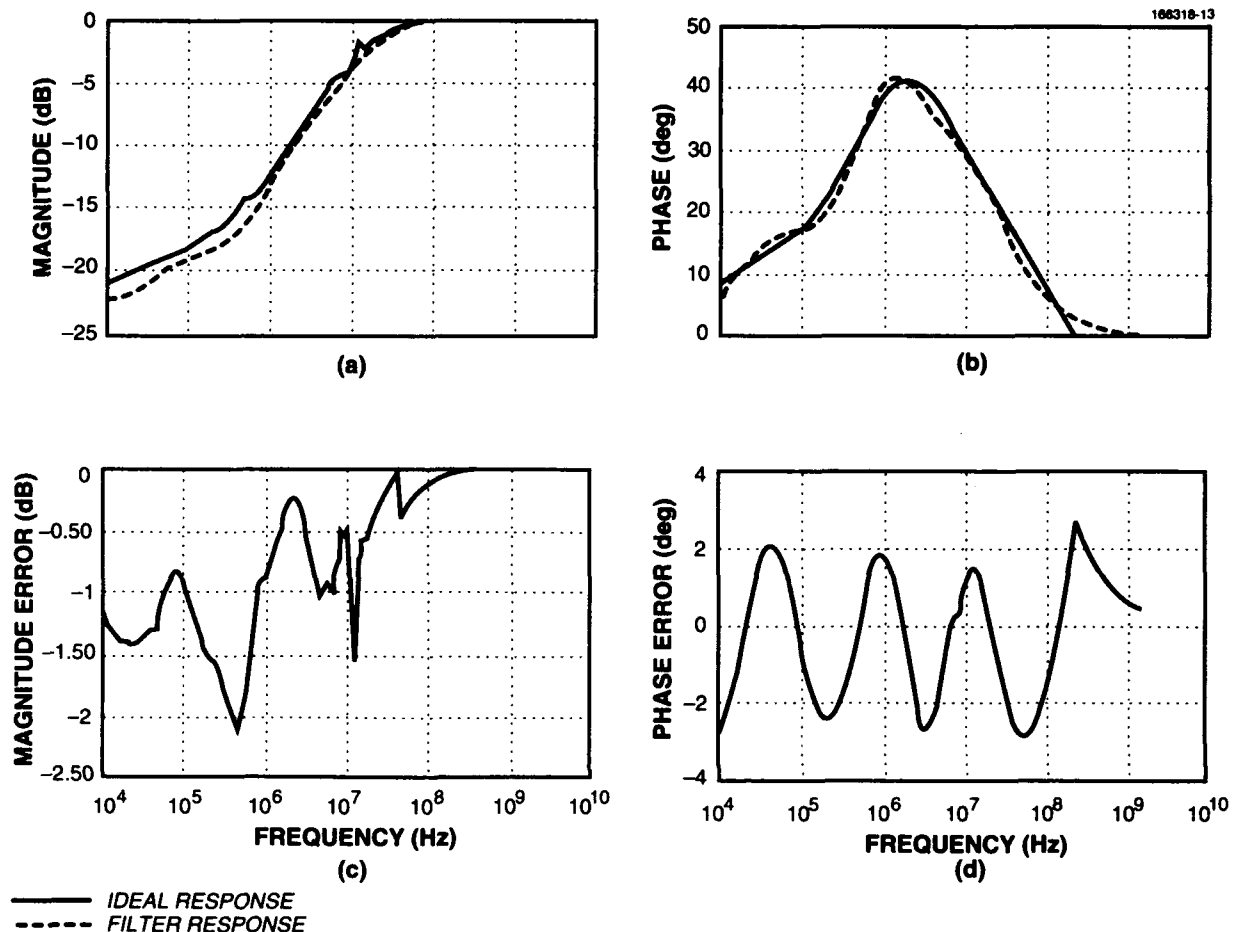


Figure 13. Optimization using equal weighting of magnitude (decibels) and phase (degrees): (a) magnitude response, (b) phase response, (c) magnitude error, and (d) phase error.

The pole and zero values resulting from the optimization were then used to synthesize a filter. Several filter topologies were considered, including constant-resistance networks such as the bridged-T and others. These networks have the advantage that they do not require a source impedance and can in fact operate from an ideal voltage or current source as shown in Figure 16(a). This operation may be an advantage in some situations where the additional voltage or current drop, which normally occurs across the source impedance, can be eliminated. Constant resistance networks can also be cascaded. The equalizer transfer function can be separated into single pole-zero pairs that can each be realized by a separate filter. The major disadvantage of constant resistance networks is their increased complexity; this was the primary reason why these networks were not preferred for this application.

The filters that have been used previously [2] are lossy, and although simpler than constant resistance networks, they use 33 percent more parts than a simple RC ladder driving-point impedance. Figures 16(b) and 17 describe the filter configuration that was used for the equalizer synthesis. These networks produce the

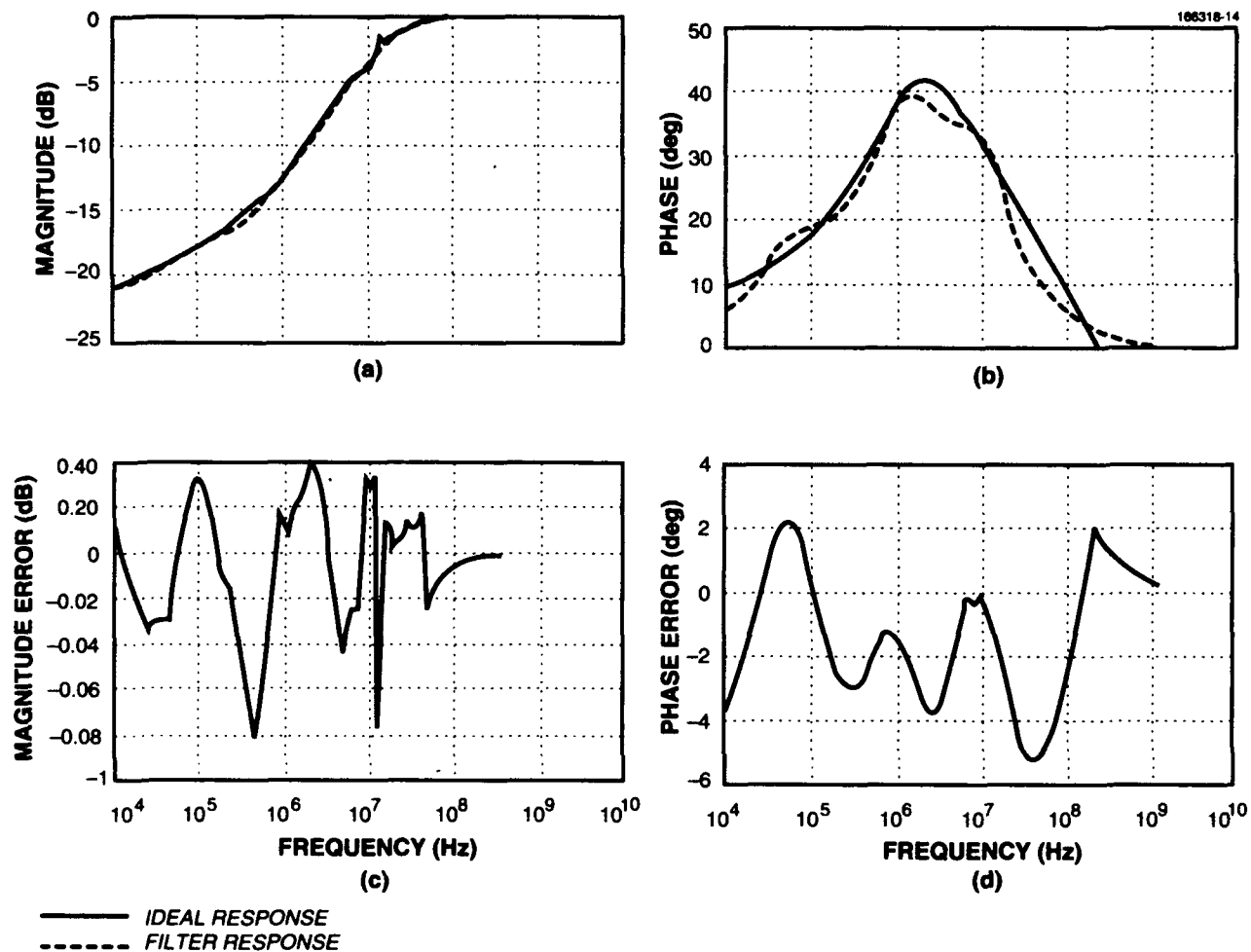


Figure 14. Optimization using optimum weighting of magnitude (decibels) and phase (degrees):  
 (a) magnitude response, (b) phase response, (c) magnitude error, and (d) phase error.

desired transfer characteristic when connected in series with a generator and load with 50-ohm impedances. They are simple to construct, use a minimum of components, and provide accurate equalization from DC to beyond 1 GHz.

The driving-point impedance is given by

$$k \cdot H_{EQ} = \frac{R_L}{R_G + R_L + Z} \quad (5.3)$$

where

$$H_{EQ} = \frac{(s + z_1)(s + z_2)(s + z_3) \dots}{(s + p_1)(s + p_2)(s + p_3) \dots} \quad (5.4)$$

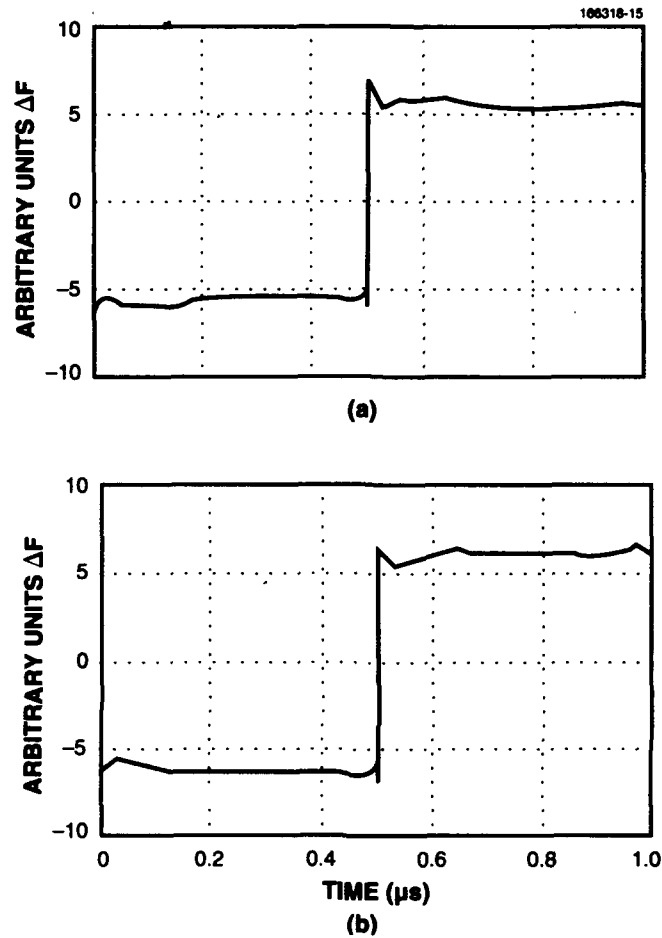


Figure 15. Calculated step response using optimized filters: (a) optimization with equal weighting of magnitude and phase ( $F = 0.129$ ) and (b) optimization with optimum weighting of magnitude and phase ( $F = 0.0755$ ).

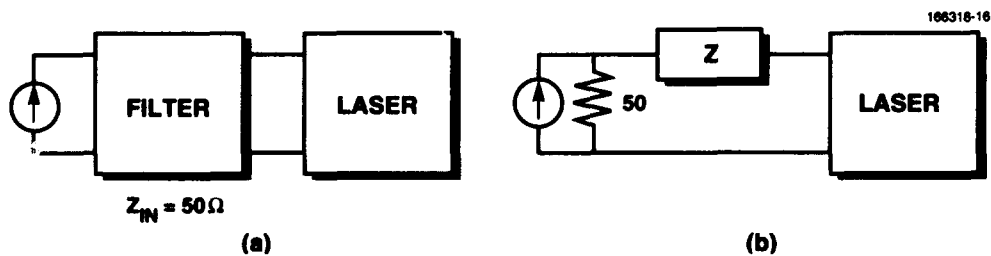


Figure 16. Filter topologies: (a) constant resistance and (b) series  $Z$ .

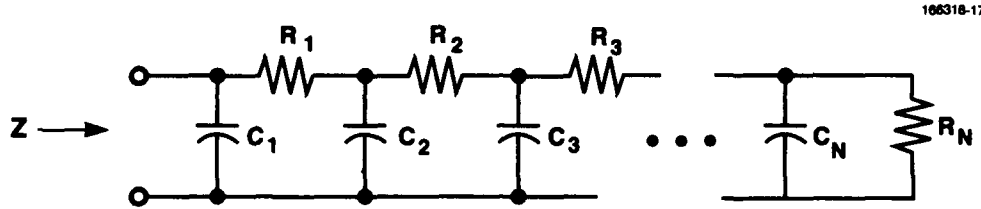


Figure 17. Series Z ladder.

Normalizing  $R_L$  and  $R_G$  to 1 ohm results in

$$k \cdot H_{EQ} = \frac{1}{2 + Z} \quad (5.5)$$

When  $Z = 0$  at high frequencies,  $H_{EQ} = 1$ , so  $k = 1/2$  and  $Z$  is given by

$$Z = \frac{2[(s + p_1)(s + p_2)(s + p_3) \dots - (s + z_1)(s + z_2)(s + z_3) \dots]}{(s + z_1)(s + z_2)(s + z_3) \dots} \quad (5.6)$$

The element values are given by the alternating partial fraction expansion of  $Y = 1/Z$ . The element values are then renormalized to 50 ohms. The resulting filter structure is shown schematically in Figure 17.

Once the element values have been calculated, the response of the equalizer filter cascaded with the laser, excited by a 1-MHz square wave, is then computed using a 2048-point IFFT to check the accuracy of the equalizer design in the time domain.

Figure 18 compares the calculated and measured performance of a laser with two-, three-, and four-pole equalization. The calculated response used an ideal 1-MHz square-wave stimulus, while the measurements show the performance with a 500-kHz square wave. Generally good agreement exists between the calculated and measured performance. However, the calculated performance shows a significant improvement between the two- and three-pole equalization, and little, if any, improvement between the three- and four-pole equalization. The measured performance, on the other hand, shows the biggest improvement between the three- and four-pole equalization. There are several possible reasons for this result.

The measurements of the FM characteristics of the lasers have some uncertainty because of phase and intensity noise in the laser output. Also, the FM characterization does not take into account the load impedance of the laser, which is assumed to be a perfect 50-ohm load. The signal source is also assumed to be a perfect 50-ohm generator. Finally, the sine-wave generator that is used for the FM measurements is not the same as the high-speed switching modulator that is used for communication experiments.

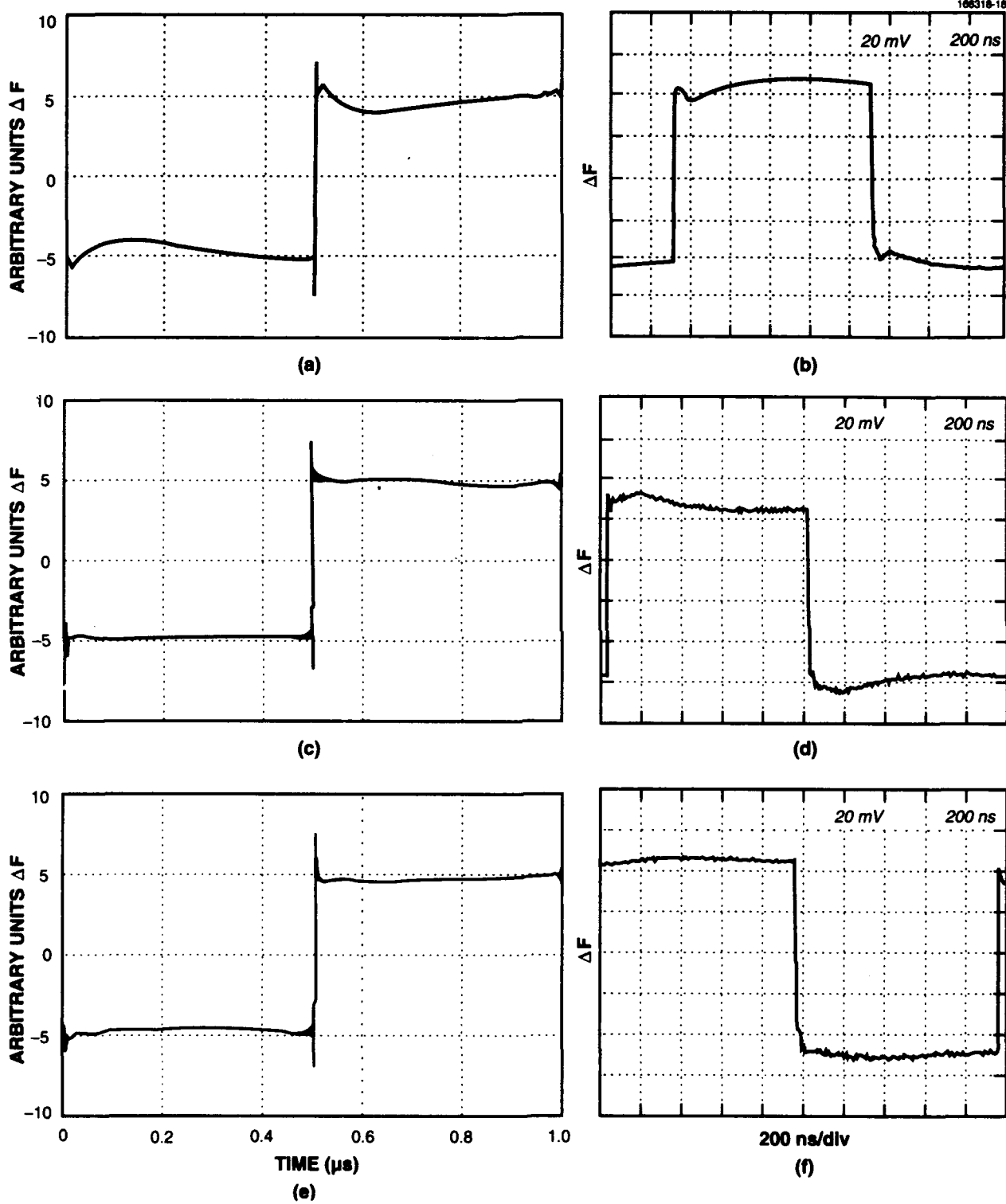


Figure 18. Equalized laser step response: (a) calculated two-pole equalizer performance, (b) measured two-pole equalizer performance, (c) calculated three-pole equalizer performance, (d) measured three-pole equalizer performance, (e) calculated four-pole equalizer performance, and (f) measured four-pole equalizer performance.

The optimization can only be as accurate as the data that is used as the optimization criteria. The series Z filter is sensitive to source and load mismatch. Therefore, although great care has been taken to minimize these potential errors, some uncertainty in the measurements remains. The components used to build the filter are not ideal and may deviate from their nominal values at high frequencies. The element values in the physical filters are somewhat constrained by available standard component values and may differ from the specified value by a few percent. The component values for a three-pole filter that was optimized for one laser are shown schematically in Figure 19(a). The actual component values are shown in Figure 19(b). A comparison between the calculated response of the circuit in Figure 19(a) and the measured response of the circuit in Figure 19(b) is shown in Table 2.

The equalizer filters were constructed on 1/16-in epoxy fiberglass printed circuit boards. The boards were designed to accommodate single- through six-pole filters on the same board. The physical board layout is shown in Figure 20. Equal path lengths were maintained through the various branches of the filter to avoid phase cancellation effects at high frequencies. The high-frequency path is kept uncluttered, passing through 50-ohm transmission lines and only one series capacitor. ATC surface mount capacitors and Allen Bradley 1/8 W, 5% carbon composition resistors were used.

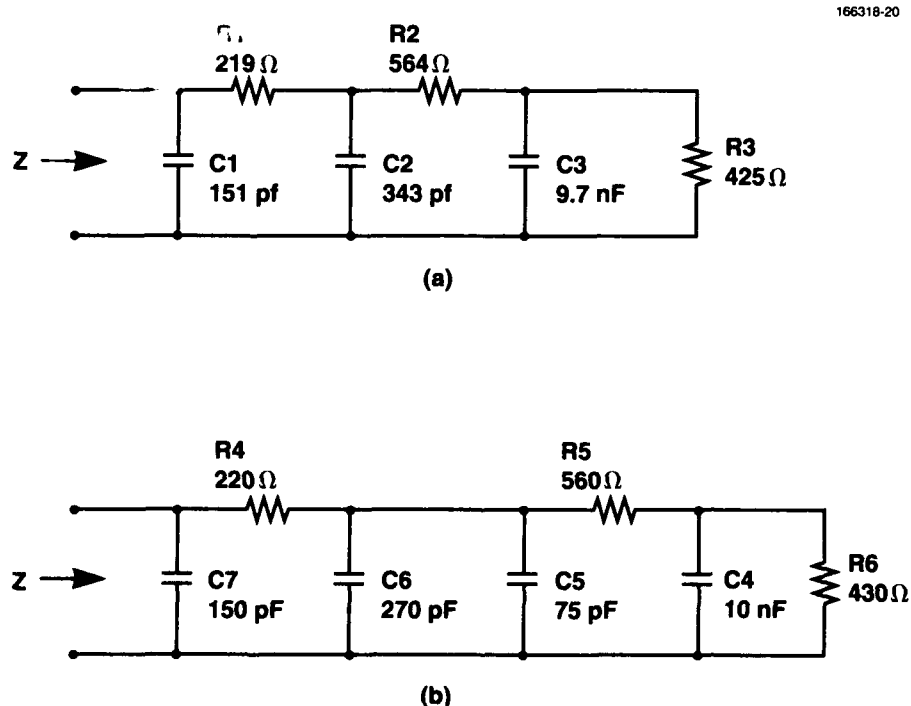
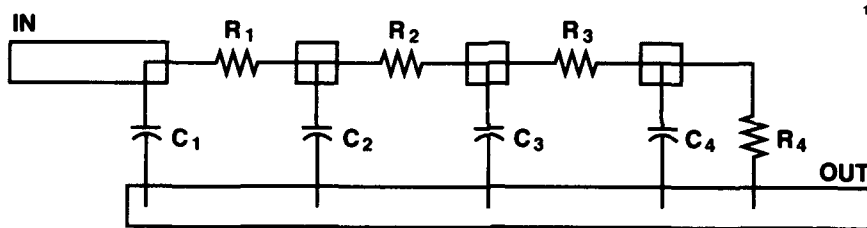


Figure 19. Element values for a three-pole equalizer: (a) optimized element values and (b) filter design using standard component values.

**TABLE 2**  
**Equalizer Filter Response**

Frequency	Calculated	Measured	Difference
10 Hz	-22.33 dB	-22.54 dB	-0.21 dB
100 Hz	-22.33 dB	-22.54 dB	-0.21 dB
1000 Hz	-22.33 dB	-22.54 dB	-0.21 dB
10000 Hz	-22.15 dB	—	—
100 kHz	-19.06 dB	-19.35 dB	-0.29 dB
1 MHz	-13.28 dB	-13.43 dB	-0.15 dB
10 MHz	- 3.93 dB	- 3.71 dB	+0.22 dB
100 MHz	- 0.09 dB	- 0.07 dB	+0.20 dB



**50  $\Omega$  MICROSTRIP**  
**CERAMIC CAPACITORS**  
**CARBON COMPOSITION RESISTORS**

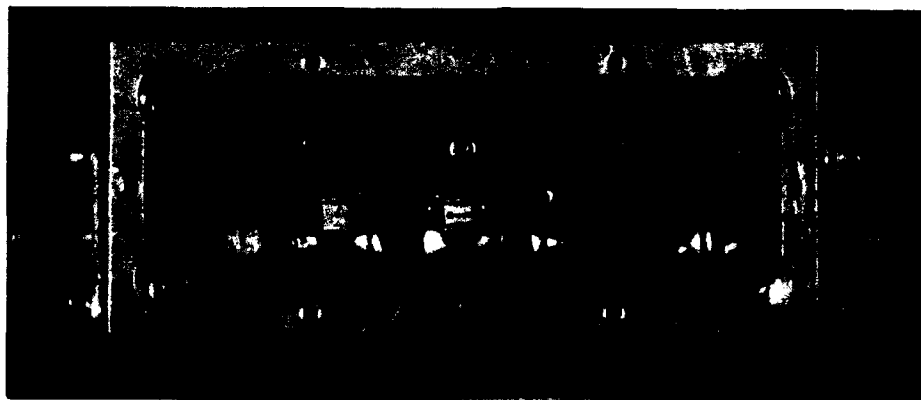


*Figure 20. Physical construction.*

## 5.2 SYSTEM PERFORMANCE

The performance of the equalized FSK communication system was measured for a transmitter laser with two- and three-pole equalization. The two-pole performance is shown in Figure 21. Figure 21(a) shows the calculated time-domain response with a 1-MHz square-wave excitation. Figure 21(b) shows an oscilloscope measurement of the actual system with a 1-MHz square wave. Excellent agreement exists between the measured and calculated waveforms.

The measured response is shown in Figures 21(c) and (d) for 10- and 100-MHz square waves. At these frequencies, the equalization is quite good even with two-pole equalization. The waveform distortion that is seen at 1 MHz would be expected to degrade the communication performance due to ISI when a long string of identical symbols is transmitted. This is indeed the case, as shown in Figures 21(e) and (f).

Figure 21(e) shows the bit error rate (BER) with a  $2^{15}-1$  pseudorandom sequence at 110 Mbit/sec. Three curves are shown. The first curve is the theoretical performance of orthogonal, noncoherent, binary FSK with a zero-linewidth source. The CSP lasers that were used in these experiments exhibited substantial phase noise that broadened the heterodyned IF linewidth to approximately 16 MHz. This linewidth noise also produces ISI, which causes the BER curve to deviate from the ideal curve at high signal-to-noise ratios (SNRs).

The effects of linewidth noise are difficult to separate from poor equalization without knowing the effect of linewidth noise alone on BER performance. The second curve in Figure 21(e), generated by a computer simulation of an FSK system with 16 MHz of linewidth noise and perfect equalization, demonstrates this effect. The third curve is the measured BER for two-pole equalization. Comparing the simulation and measured data shows that the system performance does degrade at high SNRs due to equalization errors. Further evidence is shown in Figure 21(f), which displays the measured BER performance for alternating ones and zeros at 110 Mbits/sec. The measured data and the simulation show good agreement at high SNRs in this case because the sequence of alternating ones and zeros is free of low-frequency components that are not adequately equalized.

Figure 22 shows the same laser with a three-pole equalizer. Again, there is good agreement between the calculated waveform in Figure 22(a) and the measured waveform in Figure 22(b). The absence of the initial spike seen in Figure 22(a) is likely because of low-pass parasitics in the system and measuring equipment that have filtered out some of the high-frequency energy.

The BER curves in Figures 22(e) and (f) show excellent agreement with the simulation for both a  $2^{15}-1$  pseudorandom sequence and alternating ones and zeros. This agreement indicates that the three-pole equalization is accurate enough that any errors due to equalization are well below the effects of laser linewidth noise. In the future as laser linewidth noise is reduced by the production of better laser diodes, equalization will become more critical and higher order networks may become necessary.

Figure 23 shows the effects of equalization on the time-domain performance of a pseudorandom sequence. Figure 23(a) shows the ASK waveform at the output of the modulator that drives the laser transmitter. The demodulated FM at the laser output is shown in Figure 23(b) for no equalization. There

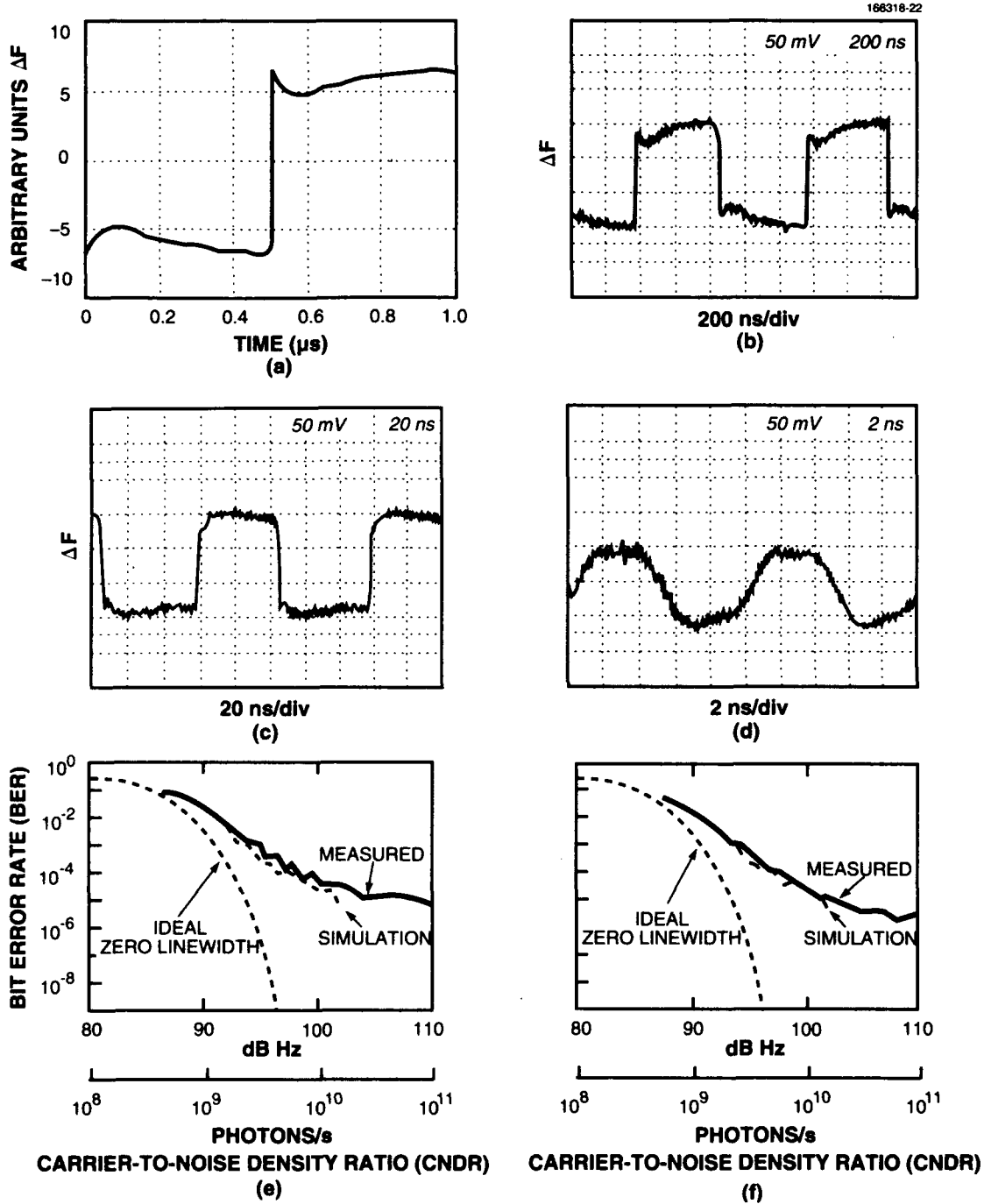


Figure 21. System performance with two-pole equalization: (a) calculated time response, (b) measured 1-MHz square-wave response, (c) measured 10-MHz square-wave response, (d) measured 100-MHz square-wave response, (e) BER at 110 Mbits/sec binary FSK with a  $2^{15}-1$  pseudorandom sequence, and (f) BER at 110 Mbits/sec binary FSK with alternating ones and zeros.

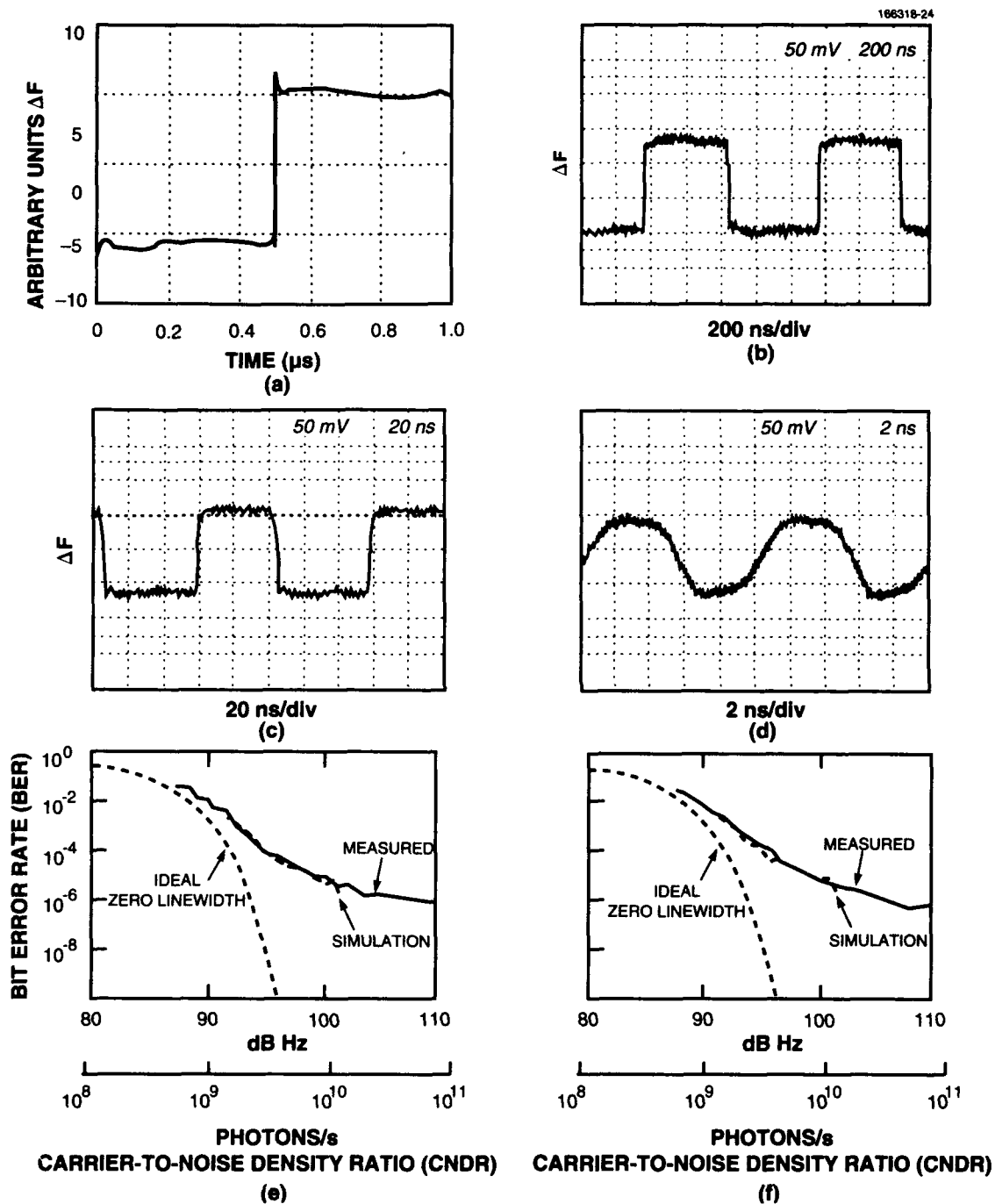


Figure 22. System performance with three-pole equalization: (a) calculated time response, (b) measured 1-MHz square wave, (c) measured 10-MHz square wave, (d) measured 100-MHz square wave, (e) BER at 110 Mbits/sec binary FSK with a  $2^{15}-1$  pseudorandom sequence, and (f) BER at 110 Mbits/sec binary FSK with alternating ones and zeros.

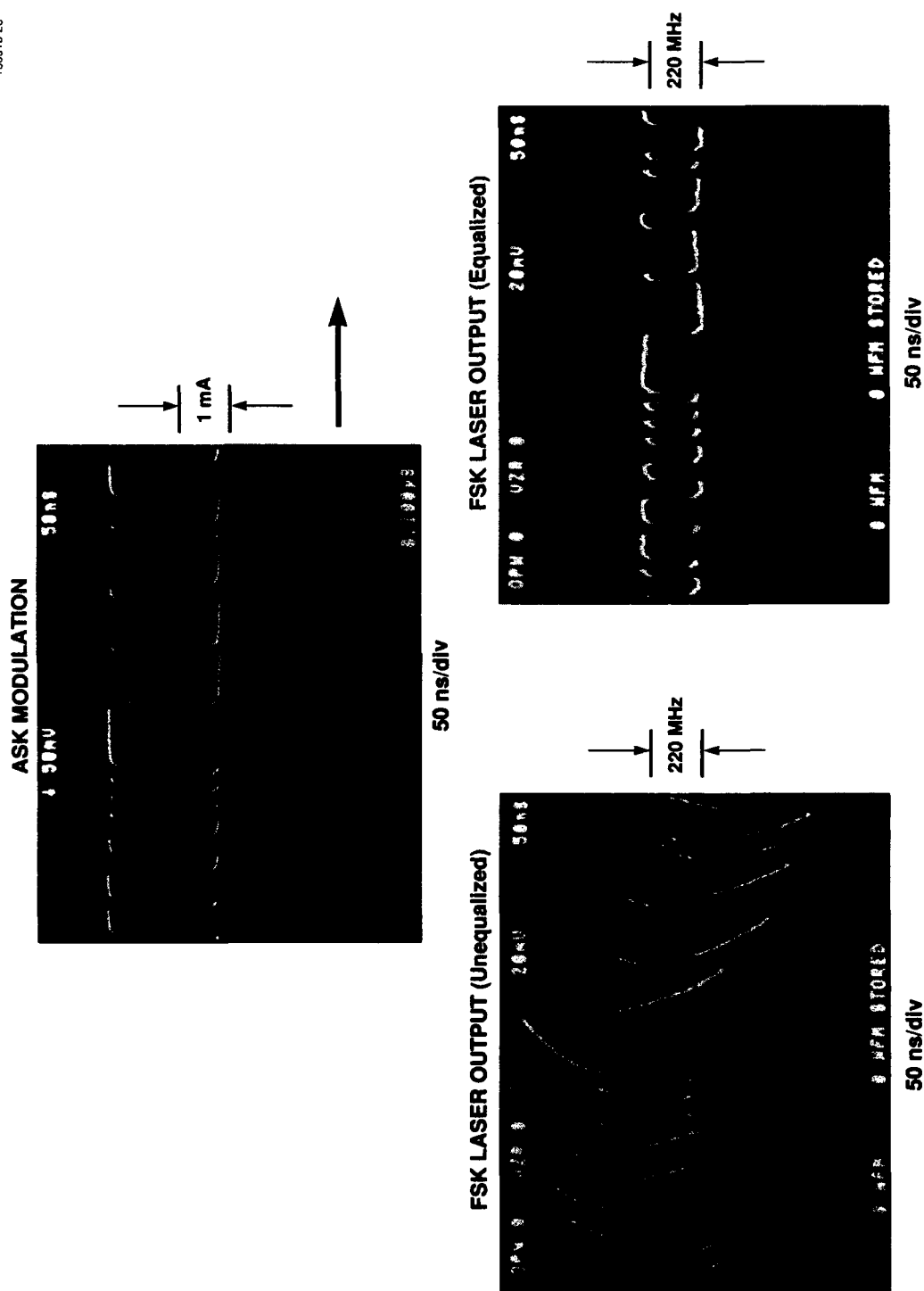


Figure 23. Laser transmitter performance: (a) ASK modulation, (b) FSK laser output (unequalized), and (c) FSK laser output (equalized).

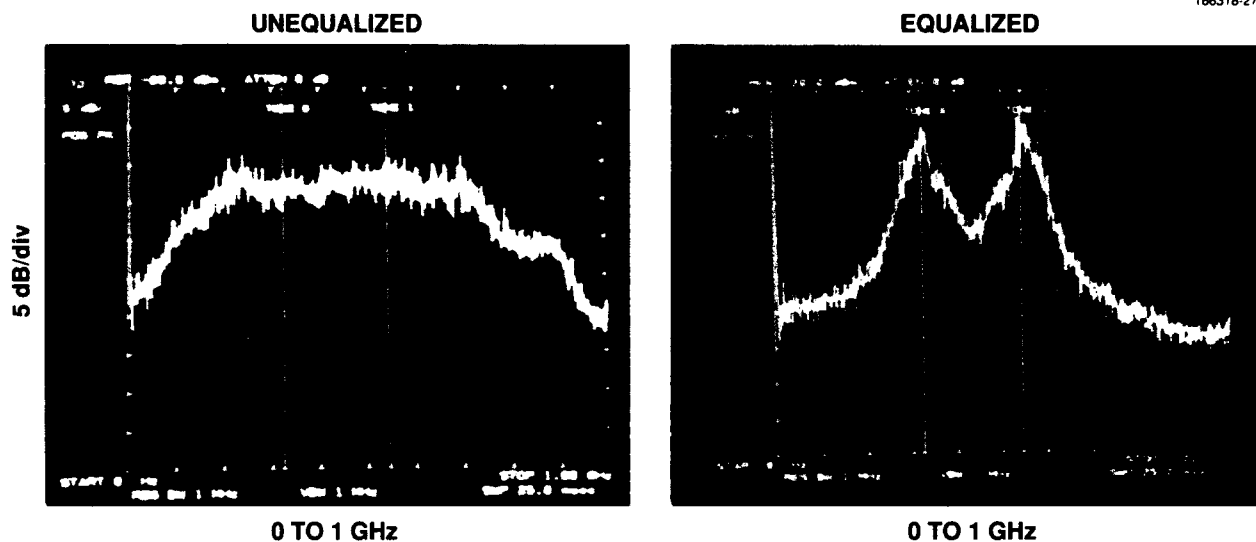


Figure 24. Laser spectra: (a) unequalized and (b) equalized.

are no distinctly spaced tones because of the FM distortion caused by the unequalized laser. The unequalized system is useless for standard FSK communication. Figure 23(c) shows the system with equalization. Now two distinct frequency tones can be demodulated with a low probability of error.

Figure 24 shows the frequency spectra of the heterodyned, FSK-modulated laser signal with a 2 x orthogonal tone spacing at 110 Mbits/sec. No distinct tones are present without equalization.

## 6. CONCLUSION

An approach to the design of passive equalization networks for wideband communication systems has been described. Several useful design tools have been developed that allow an estimate of the precision of equalization required for a specified performance in the time domain. An optimization strategy has been presented that makes use of both magnitude and phase information in the optimum way to minimize the overall error in a system transfer function. This technique has been used to design equalization networks for an FSK optical communication network with equalization requirements from DC to beyond 1 GHz. This approach has been shown to produce high-quality system equalization with low-order passive RC networks.

Much of what has been presented was specifically developed for the optical communication system problem, but the techniques and tools have broad application in such diverse areas as image rejection mixer design, adaptive antenna nulling, and other problems where two complex vectors are to be combined in an optimum way.

## APPENDIX A

### LASER EQUALIZATION PROCEDURES

The laser equalization methods follow these procedures.

(1) The FM transfer function of the laser is measured using a network analyzer that measures the difference in magnitude and phase of two voltages [3]. The network analyzer generates one of the signals internally using a frequency synthesizer. This signal is added electrically to the DC bias of the laser, causing the output of the laser to be frequency modulated at a rate determined by the input frequency. The laser output is detected using a Michelson interferometer that is set up as a delay-line discriminator. The Michelson interferometer produces a voltage output that is proportional to the sine of the phase difference between direct and delayed versions of the output of the laser. For small frequency deviations, the output varies approximately linearly with the frequency of the laser. The network analyzer compares the input signal with the output of the Michelson interferometer. The laser FM response is measured at 99 frequencies that are logarithmically spaced between 10 Hz and 1300 MHz. The instruments are controlled by an HP9836 computer that performs a calibration and records the data on a 5.25-in floppy disk.

(2) The data on the 5.25-in floppy is then transferred to the Lincoln Laboratory mainframe computer where the data is converted into a MARTHA<sup>1</sup> network. At this point, the original measured data can be recovered by printing or plotting the magnitude and phase of S21 of the network using the same frequencies at which the data was taken. MARTHA will, in addition, interpolate or extrapolate the original data for any other frequencies of interest. This capability becomes very useful later on to perform IFFTs on the measured data to construct the time-domain response of the laser cascaded onto an appropriate equalization network.

(3) A prototype equalizer response is constructed from the data produced by the laser network. (See Section 5.) The data is manually altered so that a minimum loss, minimum phase network can be constructed that will approximate the magnitude and phase function needed to equalize the laser to a flat response. The magnitude response of the filter prototype is created from the magnitude of the measured FM characteristic in decibels by multiplying by -1 and normalizing to 0 dB at the peak of the inverted response. If the laser shows a rise in the response at very high frequencies, the prototype response is forced to 0 dB at frequencies above the peak. Also, if the laser shows a sloping response above 100 MHz, the response is flattened above approximately 100 MHz.

The phase response of the prototype is subtracted from 180° to produce a minimum-phase-type response that tends to zero at DC and high frequencies. The phase response of the prototype is forced to zero at frequencies above approximately 200 MHz by the function FIXPHASE. The function FIXPHASE uses a left argument that contains the prototype filter characteristic and a right argument that is the index value of the frequency chosen for  $f_0$  in Equation (5.1). The result of FIXPHASE is a new filter characteristic where the phase values at frequencies above  $f_0$  have been replaced with the values computed by

---

<sup>1</sup> Paul Penfield, Jr., MARTHA, Massachusetts Institute of Technology (1971).

Equation (5.1). This new phase characteristic is then plotted along with the original characteristic. The right argument of FIXPHASE is iterated up or down to produce the smoothest transition from the original data to the new values. For example, EQL123B = EQL123 FIXPHASE 40.

(4) The prototype equalizer description consists of a three-dimensional array in the form of a MARTHA function of frequency (FOF). The first, second, and third columns show the magnitude in decibels, phase in degrees, and frequency in hertz, respectively. Usually, the number of rows is 63, which corresponds to the upper 63 frequencies used in the original measurement of the laser. This description is used as the variable PROTO in the APL function EQUALIZE, which in turn uses the APL function NEWT2S21, which is a Newton-Raphson optimization algorithm. NEWT2S21 uses the functions MAGNITUDEDB, PHA, and RMSARRAY. A listing of these functions is found in Appendix B.

(5) The initial guesses of the pole and zero locations are in the variable PZ, which is a vector with the zero values followed by the pole values. The optimization algorithm is usually good enough that the values used for the last optimization can generally be used as the starting point for a new design, unless the order of the filter is changed. Because PZ is a global variable, these values are normally saved after each optimization. This process eliminates the need to use a Bode plot to determine the initial guesses unless the order of the new filter is different from the order of the previous filter. The optimization can run into trouble if poor initial values are used in PZ. Two or more zeros or poles with identical values cause the error matrix to have no inverse. If instability is observed in the optimization, then new initial guesses should be derived using a Bode plot. Using too many poles and zeros can result in poor or even unstable optimization. Alternating pole and zero locations is required if the resulting function is to be realized as an RC passive network. Generally, four zeros and four poles have been found to result in the best equalization obtainable, with the accuracy that is currently available in the laser measurements.

(6) EQUALIZE requires PROTO as the left argument and PZ as the right argument. EQUALIZE prints a running account of the optimization process by scrolling information in the dialog area of the screen, which consists of a normalized error value followed by the zero and pole locations for each iteration of the optimization. The stability and accuracy of the optimization can be observed by watching that the error value does not oscillate between wildly varying values and that the pole and zero values are converging on stable values. When all of the pole and zero values are within 0.01 percent of the optimum, the optimization ceases; plots of the magnitude response, magnitude error, phase response, and phase error are drawn on the screen; the final values for the poles and zeros are printed in the dialog area. These values are also stored in the global variable PZ, which can be used in other functions to synthesize the actual equalization network. For example, RESULT = EQL123 EQUALIZE PZ. RESULT will contain the magnitude and phase of the optimized transfer function.

(7) The APL function BUILD SERIESZ uses PZ as the right argument and generates the element values for the structure shown in Figure 17. BUILD SERIESZ uses the functions EXPANDPOLY and CFRACTION. EXPANDPOLY calculates the coefficients of the polynomial whose real roots are the elements of a vector that is used as the right argument. CFRACTION performs the alternating continuous fraction expansion of the polynomial whose coefficients are the left argument, divided by the polynomial whose coefficients are the right argument. The element values calculated by BUILD SERIESZ are normalized to 1 ohm.

(8) A MARTHA network is created with the element values normalized to 50 ohms. This network can then be cascaded with the original laser network, and MARTHA can be used to analyze the total response in the frequency domain. The time-domain response of the system can be calculated using the APL function AMPLVST. AMPLVST uses the MARTHA network description as the left argument, which has been placed between single quotes, i.e., 'EQ123 WC LASER123'. The right argument is a vector that describes the input waveform. The standard test is a 1-MHz square wave described by the vector 5E-7 1 90 0 5E-7 -1 90 0 2048. AMPLVST produces a FOF that can be plotted using the standard plot functions in MARTHA. The function REAL can be used to plot the real part of the AMPLVST output. For example, PLOT REAL 'EQ123 WC LASER123' AMPLVST 5E-7 1 90 0 5E-7 -1 90 0 2048.

## APPENDIX B

### APL COMPUTER FUNCTIONS

```

VEQUALIZE[⍵]▽
[0] Z←PROTO EQUALIZE PZ;XΔLABEL;YΔLABEL;TITLEΔ;ESC
[1]  ⍵ TM←1
[2]  ESC←⍵AV[28]
[3]  ⍵←ESC,'⍵⍵2'
[4]  ⍵←ESC,'⍵⍵0'
[5]  ⍵←ESC,'⍵⍵1'
[6]  ⍵←ESC,⍵AV[13]
[7]  ⍵PW←80
[8]  Z←PROTO NEWT2S21 PZ
[9]  PICZ 1
[10] XΔLABEL←'FREQUENCY HZ'
[11] YΔLABEL←'MAGNITUDE DB'
[12] TITLEΔ←'NETWORK FREQUENCY RESPONSE'
[13] XLOGPLOT PROTO[1;;1]AND Z[;1]VS PROTO[1;;3]
[14] PICZ 2
[15] YΔLABEL←'PHASE DEG'
[16] XLOGPLOT PROTO[1;;2]AND Z[;2]VS PROTO[1;;3]
[17] PICZ 3
[18] YΔLABEL←'PHASE ERROR DEG'
[19] XLOGPLOT(Z[;2]-PROTO[1;;2])VS PROTO[1;;3]
[20] PICZ 4
[21] YΔLABEL←'MAGNITUDE ERROR DB'
[22] XLOGPLOT(Z[;1]-PROTO[1;;1])VS PROTO[1;;3]
[23] ⍵←'ZEROS ',11 -5 ⍺((⍵pz)÷2)↑pz
[24] ⍵←'POLES ',(11 -5 ⍺(-(⍵pz)÷2)↑pz),ESC,'''Δ0'
[25] ⍵ TM←0

VCFRACTION[⍵]▽
[0] C←A CFACTION B;NUMER;DENOM;D;CHAR;N;M;C1
[1]  C←10
[2]  CHAR← 5 6 ρ'÷(S×S)÷S          S      S×S  '
[3]  START:
[4]  NUMER←A
[5]  DENOM←B
[6]  →REDUCE×1B[1]=0
[7]  C1←A[1]÷B[1]
[8]  C←C,C1
[9]  N←ρA
[10] M←ρB
[11] ⍵←(⍺C1),',',,CHAR[(3+N-M);]
[12] D←C1×DENOM
[13] D←D,0×1(N-M)
[14] A←DENOM
[15] B←NUMER-D
[16] REDUCE:
[17] B←1÷B
[18] →START×1(ρB≠0)

```

```

[0] B←NET AMPLVST A;ΔT;N1;N2;ΔF;FR;A1;A2;SIG;F;FRM;DC1;DC2
[1] DC2←DC1+0
[2] IN:→(9=ρ,A)/START
[3] →DCPRAM×111=ρ,A
[4] B←B←'ENTER FIRST SIGNAL PARAMETERS AS T1,A1,DEG1,F1,DC1: '
[5] A←*(ρB)↓B
[6] B←B←'ENTER SECOND SIGNAL PARAMETERS AS T2,A2,DEG2,F2,DC2: '
[7] A←A,*(ρB)↓B
[8] B←B←'ENTER NO. OF POINTS: '
[9] A←A,*(ρB)↓B
[10] →IN
[11] DCPRAM:DC1+A[5]
[12] DC2←A[10]
[13] A←A[1 2 3 4 6 7 8 9 11]
[14] AZERO TAME TO FREE WORKSPACE
[15] START:TAME←10
[16] ACHANGE NO. OF POINTS TO A PWR OF 2
[17] A[9]←2*[(A[9])÷2
[18] ASAVE INPUT 'A' IN BACKGROUND VAR
[19] AA←A
[20] ACOMPUTE TIME AND FREQ PARAMETERS
[21] ΔT←(A[1]+A[5])÷A[9]
[22] N2←10.5+A[9]×A[5]÷A[1]+A[5]
[23] N1←A[9]-N2
[24] ΔF←A[1]+A[5]
[25] APCOPY IN MARTHA FNS
[26] 1 COPYΔWS 'MARTHADH'
[27] ADEFINE MEASUREMENT FREQUENCIES
[28] F←ΔF×1E-10,1A[9]÷2
[29] ACOMPUTE NETWORK RESPONSE
[30] FR←((ρF),3)ρVG OF*,NET
[31] AZERO OUT MARTHA HEADER (hd)
[32] hd←10
[33] AMAKE INTO A COMPLEX VECTOR AND ALIGN WITH SIG FFT
[34] ATHAT IS FIRST ELEMENT IS ZERO FREQ
[35] FRM←(1 0)↓(1 0)↓ρFR
[36] FRM[; 2 3]←FRM[; 2 3]
[37] FR←FR,[1]FRM
[38] FR←ρFR[; 1 2]
[39] ACOMPUTE TEST SIGNAL PHASE IN RADIANs
[40] A1←(0A[3]÷180)+02×A[4]×ΔT×-1+1N1
[41] A2←(0A[7]÷180)+02×A[8]×-ΔT×1+N2-1N2
[42] ACOMPUTE COMPLEX TEST SIGNAL
[43] SIG←(2,A[9])ρ((A[2]×10A1)+DC1),((A[6]×10A2)+DC2),A[9]ρ0
[44] ACOMPUTE COMPLEX TIME RESPONSE
[45] B←IFFT FR XTIME FFT SIG
[46] APUT IN TEK PLOT FORMAT, COL 1,2=RESPONSE, COL3=SIG, COL4=TIME
[47] ARESPONSE=RE(B),IM(B); SIG=RE(SIG)
[48] B←*(4,A[9])ρ(,B),SIG[1;],ΔT×-1+1A[9]
[49] APUT B IN VAR TAME FOR FUTURE USE IF REQUIRED
[50] TAME←B

```

```

      VNEWT2S21[ ]V
[0] H←FT NEWT2S21 PZ;MB;AB;EI;E0;E2;E3;E4;J;ERROR;N;I;P;EM;EA;JM;JA;DN
[1] N←ρPZ
[2] ERROR←10
[3] MB←FT[;;3]MAGNITUDEDB PZ
[4] AB←FT[;;3]PHA PZ
[5] H←Φ(2,(ρFT)[2])ρMB,AB
[6] EI←FT RMSARRAY H
[7] E0←(+EI)÷ρEI
[8] Q←12-5 *E0,PZ
[9] LOOP:P←PZ
[10] K←2
[11] EM←(FT[1;;1]-,MB)×0.978×40÷10
[12] EM←EM°.×((N÷2)ρ-1),(N÷2)ρ1
[13] EA←(FT[1;;2]-,AB)×0.022×2×180÷01
[14] EA←EA°.×((N÷2)ρ1),(N÷2)ρ-1
[15] DN←((02×FT[1;;3])*2)°.+P*2
[16] JM←(((ρFT)[2])ρ1)°.×P÷DN
[17] JA←((02×FT[1;;3])°.×(Nρ1))÷DN
[18] ERROR←(EM×JM)+(EA×JA)
[19] ERROR←EI#ERROR
[20] STEP:K←K÷2
[21] P←P-K×ERROR
[22] MB←FT[;;3]MAGNITUDEDB P
[23] AB←FT[;;3]PHA P
[24] H←Φ(2,(ρFT)[2])ρMB,AB
[25] E4←FT RMSARRAY H
[26] E3←(+E4)÷ρE4
[27] Q←12-5 *E3,P
[28] →CONT×1E3≤E0
[29] P←P+K×ERROR
[30] →STEP
[31] CONT:→QUIT×1×/(1(PZ-P)÷PZ)<(Nρ1E-4)
[32] E0←E3
[33] PZ←P
[34] EI←E4
[35] ERROR←10
[36] →LOOP
[37] QUIT:MB←FT[;;3]MAGNITUDEDB PZ
[38] AB←FT[;;3]PHA PZ
[39] H←Φ(2,(ρFT)[2])ρMB,AB
[40] pZ←PZ

```

```

      VPHA[ ]V
[0] Z←PH PHA SN;Z1;Z2
[1] N←ρSN
[2] Z1←(N÷2)†SN
[3] Z2←(-N÷2)†SN
[4] Z←+/-3002×PH°.×÷Z1
[5] Z←Z-+/-3002×PH°.×÷Z2
[6] Z←Z×180÷01

```

```

      VRMSARRAY[ ]V
[0] Z←EXACT RMSARRAY TEST
[1] Z←0.978×(((, EXACT[1;;1])−TEST[;1])×2)
[2] Z←Z+0.022×(((, EXACT[1;;2])−TEST[;2])×2)

      VBUILDSERIESZ[ ]V
[0] Z←BUILDSERIESZ PZ;A;B;N
[1] N←ρPZ
[2] A←EXPANDPOLY(−N÷2)↑PZ
[3] B←EXPANDPOLY(N÷2)↑PZ
[4] A←2×(A−B)
[5] Z←A CFRACTION B

      VEXPANDPOLY[ ]V
[0] Z←EXPANDPOLY S;N;I
[1] N←ρS
[2] I←1
[3] Z←1, S[1]
[4] LOOP:I←I+1
[5] →0×1 I>N
[6] Z←(1, S[I])°×Z
[7] Z←Z, [2]2ρ0
[8] Z←(0 −1)ΦZ
[9] Z←+Z
[10] →LOOP

      VFIXPHASE[ ]V
[0] Z←FT FIXPHASE F0;F1
[1] F1←F0−4
[2] F1←F1+1(63−F1)
[3] FT[1;F1;2]←45−180×(−3°(FT[1;F1;3]÷FT[1;F0;3]))÷02
[4] Z←FT

      VMAGNITUDEDB[ ]V
[0] Z←FR MAGNITUDEDB PZ
[1] N←ρPZ
[2] FR←FR÷100000
[3] PZ←PZ÷100000
[4] PZ←PZ×2
[5] Z←×/((02×FR)×2)°+ (N÷2)↑PZ
[6] Z←Z÷×/((02×FR)×2)°+ (−N÷2)↑PZ
[7] Z←10×10°Z

```

## REFERENCES

1. L.O. Chua and P-M. Lin, *Computer-Aided Analysis of Electronic Circuits: Algorithms and Computational Techniques*, Englewood, NJ: Prentice Hall Inc. (1975), p. 218.
2. S.B. Alexander et al., "Passive equalization of semiconductor diode laser frequency modulation," *J. Lightwave Technol.* **LT-7**, 11-23 (1989).
3. D. Welford and S.B. Alexander, "Magnitude and phase characteristics of frequency modulation in directly modulated GaAlAs semiconductor diode lasers," *J. Lightwave Technol.* **LT-3**, 1092-1099 (1985).

REPORT DOCUMENTATION PAGE			Form Approved OMB No. 0704-0188	
<small>Public reporting burden for this collection of information is estimated to average 1 hour per response, including the time for reviewing instructions, searching existing data sources, gathering and maintaining the data needed, and completing and reviewing the collection of information. Send comments regarding this burden estimate or any other aspect of this collection of information, including suggestions for reducing this burden, to Washington Headquarters Services, Directorate for Information Operations and Reports, 1215 Jefferson Davis Highway, Suite 1204, Arlington, VA 22202-4302, and to the Office of Management and Budget, Paperwork Reduction Project (0704-0188), Washington, DC 20503.</small>				
1. AGENCY USE ONLY (Leave blank)	2. REPORT DATE 22 March 1991	3. REPORT TYPE AND DATES COVERED Technical Report		
4. TITLE AND SUBTITLE  Passive Equalization of Wideband Communication Systems		5. FUNDING NUMBERS  C — F19628-90-0002 PR — 270		
6. AUTHOR(S)  Mark L. Stevens				
7. PERFORMING ORGANIZATION NAME(S) AND ADDRESS(ES)  Lincoln Laboratory, MIT P.O. Box 73 Lexington, MA 02173-9108		8. PERFORMING ORGANIZATION REPORT NUMBER  TR-909		
9. SPONSORING/MONITORING AGENCY NAME(S) AND ADDRESS(ES)  Air Force Space Technology Center (AFSTC/SWL) Kirtland AFB, NM 87117-6008		10. SPONSORING/MONITORING AGENCY REPORT NUMBER  ESD-TR-90-146		
11. SUPPLEMENTARY NOTES  None				
12a. DISTRIBUTION/AVAILABILITY STATEMENT  Approved for public release; distribution is unlimited.			12b. DISTRIBUTION CODE	
13. ABSTRACT (Maximum 200 words)  <p>This report describes a technique that produces high-performance passive equalization networks for wideband communication systems. The relationship between the time-domain and frequency-domain performance of a simple but important class of networks is derived. The results of this analysis provide an estimate of the precision of equalization required in the frequency domain, given the requirements for waveform quality in the time domain. The effects of equalization magnitude and phase errors on a system transfer function are described, and the optimum weighting function for the least-mean-square-error minimization of magnitude and phase errors is derived. An example is given of the baseband equalization of a 220-Mbit/sec 4-ary FSK optical communication system. High-quality equalization is achieved using this technique over a frequency range of DC to approximately 1 GHz using simple, economical networks. Appendices are provided that describe the APL computer functions that were written to optimize and synthesize the filter hardware.</p>				
14. SUBJECT TERMS equalization                      optimization                      optical filter                                  laser                                  coherent communication                      frequency-shift-key (FSK)			15. NUMBER OF PAGES 62	
			16. PRICE CODE	
17. SECURITY CLASSIFICATION OF REPORT  Unclassified	18. SECURITY CLASSIFICATION OF THIS PAGE  Unclassified	19. SECURITY CLASSIFICATION OF ABSTRACT  Unclassified	20. LIMITATION OF ABSTRACT	